Landslide Susceptibility Mapping using GIS-based Frequency Ratio and Shannon Entropy, in part of Chamoli district, Uttarakhand, India

A DISSERTATION

SUBMITTED IN PARTIAL FULFILLMENT OF THE
REQUIREMENT FOR THE AWARD OF THE DEGREE OF

MASTER OF TECHNOLOGY

IN

GEOTECHNICAL ENGINEERING

Submitted by:

DHRUV BHARDWAJ

(2K20/GTE/07)

Under the Supervision of

PROF. RAJU SARKAR

DEPARTMENT OF CIVIL ENGINEERING

DELHI TECHNOLOGICAL UNIVERSITY

(Formerly Delhi College of Engineering)

Bawana Road, Delhi-110042

MAY 2022

DEPARTMENT OF CIVIL ENGINEERING

DELHI TECHNOLOGICAL UNIVERSITY

(Formerly Delhi College of Engineering)

Bawana Road, Delhi-110042

CANDIDATE'S DECLARATION

I, Dhruv Bhardwaj, Roll No – 2K20/GTE/07, a student of M.Tech. in Geotechnical Engineering, declare that the project Dissertation titled "Landslide susceptibility mapping using GIS-based Frequency Ratio (FR) and Shannon Entropy in part of Chamoli district, Uttarakhand, India" which is submitted by me to the Department of Civil Engineering, Delhi Technological University, Delhi for the partial fulfillment of the requirement for the award of the degree of Master of Technology, is original and not copied from any source without proper citation. This work has not previously formed the basis for the award of any Degree, Diploma Associateship, Fellowship or other similar title or recognition.

Place: Delhi

DHRUV BHARDWAJ

Date: 20.05.2022

DELHI TECHNOLOGICAL UNIVERSITY

(Formerly Delhi College of Engineering)

Bawana Road, Delhi-110042

CERTIFICATE

I hereby certify that the Project Dissertation titled “Landslide susceptibility mapping using GIS-based Frequency Ratio and Shannon Entropy approaches in part of Chamoli district, Uttarakhand, India” which is submitted by Dhruv Bhardwaj; Roll No – 2K20/GTE/07; Department of Civil Engineering, Delhi Technological University, Delhi for the partial fulfillment of the requirement for the award of the degree of Master of Technology, is a record of the project work carried out by the student under my supervision. To the best of my knowledge, this work has not been submitted in part or full for any Degree or Diploma to this University or elsewhere.

Place: Delhi **PROF. RAJU SARKAR**

Date: 20.05.2022 **SUPERVISOR**

ABSTRACT

Landslides are one of the most adverse naturally or artificially occurring hazards that results in a great loss to life and property across the globe. Moreover, people living in the upside of landslide completely lose their access to the basic amenities like: markets, food, schools, hospitals, etc. with a fear of upcoming danger of another landslide event.

Therefore, it becomes essential to determine areas which are most likely to get affected by landslides, for ensuring risk mitigation and disaster resilient planning of infrastructure projects by government and private entities involved in construction projects. This study aims at evaluating the effectiveness of two GIS-based statistical approaches namely, Frequency ratio (FR) and Shannon Entropy (SE) for the landslide susceptibility mapping of a region in Chamoli district, in Uttarakhand, India. There are a lot of ongoing and proposed infrastructure projects in the area due to which, there is a surge in tourism in the area. A total of ten landslide factors which directly or indirectly influence the landslide occurrence are considered in this research study namely: elevation, slope, aspect, curvature, lithology, distance to roads, distance to faults/lineaments, distance to river, topographic wetness index, and stream power index. The landslide inventory data (from 2005-2019) has been prepared from Bhukosh Portal by Geological Survey of India in point shapefile format. The obtained dataset for landslide inventory was then randomly divided into training (80%) and testing (20%) datasets. The relationship existing between landslide points and the taken landslide causative factors has been validated through the application of the incorporated models. A total of two landslide susceptibility maps were prepared from the outputs of this research work and were validated through Area Under Curve (AUC) of Receiver Operator Characteristics (ROC) curve. The resultant maps from this research study can be extremely

useful for the planners and designers from similar areas for ensuring a safe and disaster resilient infrastructure against a destructive natural calamity like landslide.

ACKNOWLEDGEMENTS

The following research work is the final output of my two years master's degree in Geotechnical Engineering at the Delhi Technological University (DTU), New Delhi, India. I would like to express my heartfelt appreciation to the staff of Delhi Technological University (DTU) for their prompt academic and administrative support, without which this work would not have been successful.

I am grateful to my thesis supervisor, Prof. Raju Sarkar for his valuable guidance and constructive scholarly suggestions during the planning and implementation of my project work. Without his timely inputs and periodic assessments, this project would not have given the desired results.

I would like extend my heartfelt appreciation to my family members for their constant encouragement and support for the completion of the course. I would also like to thank my friends in the college throughout the study programme with whom I gained valuable experiences through which I tried to dive into the deep sea of knowledge.

DHRUV BHARDWAJ

TABLE OF CONTENTS

CANDIDATE'S DECLARATION ..... **ii**

CERTIFICATE ..... **iii**

ABSTRACT ..... **iv**

ACKNOWLEDGEMENTS ..... **vi**

List of Tables ..... **x**

List of Figures ..... **xi**

CHAPTER 1 INTRODUCTION **1**

1.1 Background and motivation of research 1

1.2 Aims of research work 2

1.3 Objectives 2

CHAPTER 2 LITERATURE REVIEW **4**

2.1 Overview of research carried out 4

2.2 Definitions and types of landslides 4

2.3 Remote sensing software-Geographic Information System (GIS) and it's applications 6

2.4 Landslide identification and mapping 7

CHAPTER 3 STUDY AREA 10

3.1 Uttarakhand 10

3.2 Chamoli District 11

CHAPTER 4 METHODOLOGY AND DATABASE PREPARATION 13

4.1 Methodology adopted 13

4.2 Data used 14

4.3 Derivatives obtained from DEM 15

4.3.1 Slope 16

4.3.2 Aspect 16

4.3.3 Curvature 17

4.3.4 Elevation 18

4.3.5 Topographic Wetness Index (TWI) 19

4.3.6 Stream Power Index (SPI) 20

4.4 Other prepared thematic layers 21

4.4.1 Distance to roads 21

4.4.2 Distance to faults/lineaments 22

4.4.3 Lithology 23

4.4.4 Distance to river 25

4.5 Landslide Inventory map 25

4.5.1 Random splitting of samples 26

CHAPTER 5 ADOPTED PROBABILITY APPROACHES: CONCEPTS AND COMPUTATION RESULTS 27

5.1 Statistical methods incorporated in the study 27

5.1.1 Frequency Ratio (FR) concept 27

5.1.2 Shannon Entropy (SE) 28

5.2 Computation results 29

CHAPTER 6 RESULTS AND DISCUSSIONS 44

6.1 Landslide Susceptibility Map (LSM) Generation and classification 44

6.2 Validation results 45

6.2.1 Area Under the Curve (AUC) of Receiver Operator Characteristics (ROC) curve 45

CHAPTER 7 CONCLUSION AND LIMITATION 48

7.1 Conclusion 48

7.2 Limitations 49

REFERENCES 50

LIST OF TABLES

Table 2.1 Types of landslides 5

Table 4.1 Data used and their various sources 15

Table 5.1 Frequency Ratio results for each landslide causative factor 30

Table 5.2 Prediction Rate for each landslide causative factor 35

Table 5.3 Results of Shannon Entropy 36

Table 5.4 Individual weights for each landslide causative factor (SE) 43

Table 6.1 Summary of ROC results for FR and SE 46

LIST OF FIGURES

Fig. 2.1 Block diagram of idealized landslide-earth flow (Varnes, 1978) 5

Fig. 3.1 Uttarakhand State map 10

Fig. 3.2 Chamoli district map (*Source: Chamoli District Website | India*) 11

Fig. 4.1 Flow Chart of the methods involved 13

Fig. 4.2 Slope map 16

Fig. 4.3 Aspect map 17

Fig. 4.4 Curvature map 18

Fig. 4.5 Elevation map 18

Fig. 4.6 Topographic Wetness Index (TWI) map 19

Fig. 4.7 Stream Power Index (SPI) map 20

Fig. 4.8 Distance to road map 21

Fig. 4.9 Distance to faults/lineaments map 22

Fig. 4.10 Lithology map 23

Fig. 4.11 Distance to river map 25

Fig. 4.12 Training and testing datasets 26

Fig. 6.1 Landslide Susceptibility Map for Frequency Ratio (FR) model 44

Fig. 6.2 Landslide Susceptibility Map (LSM) for Shannon Entropy (SE) model 45

Fig. 6.1.1 Success rate curves for the FR and SE models..... 46

Fig. 6.1.2 Prediction rate curves for the FR and SE models..... 47

CHAPTER 1-INTRODUCTION

1.1 Background and motivation of research:

Landslides cause widespread destruction of life and property. A lot of ongoing infrastructure projects come to halt due to the landslide occurrence. Between 1998-2007, nearly 4.8 million people across the globe were affected by landslides with an estimated death count of 18000. The complex nature of landslides has made it quite a challenging task to study. It involves an extensive collaboration of different domains for an efficient prediction and mitigation. Hence, the results produced by landslide susceptibility maps can be of great use.

India is one of the most affected countries by landslides, particularly in the Himalayan region due to their relatively young age, claiming more than 3000 lives from 2010-to 2019 (Statista.com). Due to their young age, the Himalayan range is characterized by unstable geology having major faults. Other anthropogenic factors along with the construction activities like dams, power projects, etc. further increase the likelihood of landslide occurrence.

Uttarakhand, also known as Devbhumi (land of Gods) is one of the most vulnerable states to the landslide occurrence in India. Tourism in the state has increased manifolds, which increases the need to develop infrastructure as well as other developmental works like road widening, hotels, power projects, etc. Such developmental projects improve the overall connectivity and bring prosperity and upliftment to an area. However, they increase the risk of instability in slopes due to which, the likelihood of landslide occurrence increases. Landslide mapping has been done in many areas. However, the factors taken in this research study along with the application of applied models in this research study have not been analyzed before for the Chamoli district in Uttarakhand.

1.2 Aims of research work:

This research study aims to classify the taken study area in distinctive landslide susceptibility classes through the incorporation of statistical models using a total of ten landslide causative factors. After the application of these models, the investigation aims to establish the suitability of the application of incorporated models in the Chamoli district.

The findings of this research work will also be beneficial for creating awareness for ensuring a disaster resilient infrastructure against landslides, which can be a lifesaver in similar areas as well.

1.3 Objectives:

The main research objectives formulated for this research work have been outlined as:

- To understand the landslide-prone points in the taken area extensively, a thorough literature review of similar research projects across India and the globe where similar or different landslide causative factors were utilized.
- To create a landslide inventory map for the area in order to gain a sense of the previously occurred landslides and using it to create landslide susceptibility maps for future landslide prediction.
- To create a distinctive thematic map for each included landslide causative factor that were considered in this research on Geographic Information System (GIS) platform ArcMap.
- Producing landslide susceptibility maps using Frequency ratio and Shannon Entropy models and their corresponding prediction rates and then, classifying various landslide susceptibility zones in the study area.
- Validating the models involved in the creation of the map using the Area under curve (AUC) approach of the Receiver Operating Characteristic (ROC) curve for both the training and testing dataset of landslide inventory.

The most important aspect of this research project is the inventory map for the landslides that have previously occurred in this area. They were thoroughly recorded, identified and analyzed. Then, the aforementioned models were applied and based on the applied models, landslide susceptibility maps were generated for the prediction of future landslides in the Chamoli District in Uttarakhand.

CHAPTER 2-LITERATURE REVIEW

2.1 Overview of research carried out:

For ensuring the prevention of losses that occurred due to landslide hazards, landslides must be monitored and this has become an area of great interest across the globe. The principal reason behind this unprecedented growth is the number of research projects and publications globally.

The nature of the landslides occurring in different areas is highly complex with a number of causative factors which affect the occurrence of landslides directly or indirectly. The applicability of different prediction methods varies for different sets of landslide causative factors which require extensive field surveys as well as site investigation. Therefore, landslide susceptibility mapping through soft computational skills as well as the incorporation of software-based techniques. Similar to them, this research work is a contribution to ensuring proper and timely preventive measures which will mitigate the risk of landslide occurrence. Finally, a landslide zonation map showing different susceptibility zones will be produced based on the taken factors and the results were validated.

2.2 Definition and Types of Landslides:

Landslides are classified as an occurrence of an event in which rock mass, debris, or soil travels down the slope. It's mechanism is characterized by slide, flow or fall of materials under the influence of gravitational pull acting downward the slope (Das 2011; Motamedi 2013). Due to the sheer complexity of the nature of landslides, it was quite difficult for the scientists to come to a common definition for the landslide. For determining the areas susceptible to a higher risk of landslide occurrence, a detailed analysis of landslides that have occurred historically in the area is crucial. This is because the areas which are most likely to be affected by the occurrence of landside disasters will also be susceptible to the occurrence of landslide events in the future. The tools present in Geographic Information System (GIS) can be utilized for an effective and accurate mapping of previously occurred landslides (Audisio et al. 2009; Mandal and Mondal 2019; Yalcin 2008; Yalcin et al. 2011; Yilmaz and Keskin 2009).

There are several types of landslides that were thoroughly described by Varnes, 1978. They are represented in Table 1:

Table 2.1: Types of landslides. Abbreviated version of Varnes' classification of slope movements (Varnes, 1978)

TYPE OF MOVEMENT		TYPE OF MATERIAL		
		BEDROCK	ENGINEERING SOILS	
			Predominantly coarse	Predominantly fine
FALLS		Rock fall	Debris fall	Earth fall
TOPPLES		Rock topple	Debris topple	Earth topple
SLIDES	ROTATIONAL	Rock slide	Debris slide	Earth slide
	TRANSLATIONAL			
LATERAL SPREADS		Rock spread	Debris spread	Earth spread
FLOWS		Rock flow (deep creep)	Debris flow (soil creep)	Earth flow
COMPLEX		Combination of two or more principal types of movement		

There are various parts of a landslide hazard which are shown in Figure 2.1.

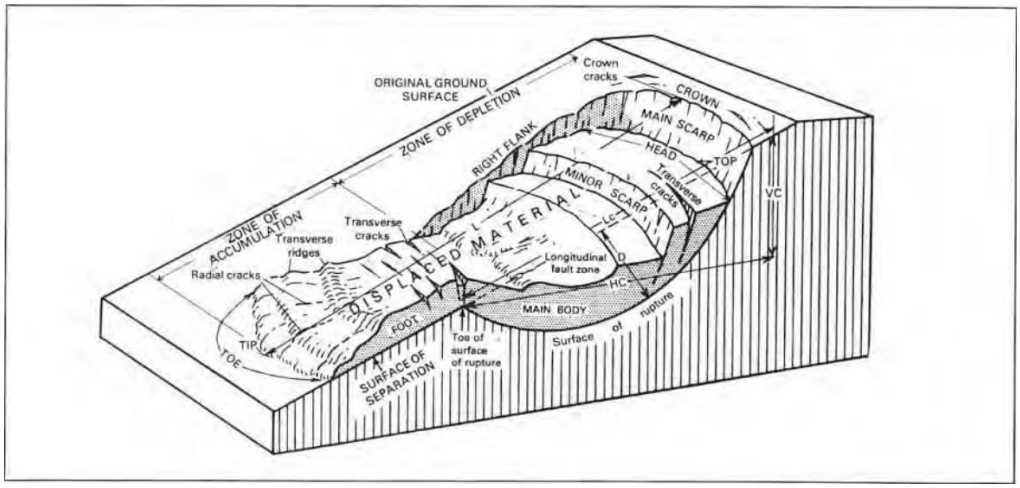

Fig 2.1: Block diagram of idealized landslide-earth flow (Varnes, 1978)

Cruden and Varnes (1996) specified various factors that result in the occurrence of landslide disasters. They can be of various types such as geological, morphological, physical and anthropogenic. They initiate the landslide occurrence either directly or indirectly. Sometimes,

some artificial/man-made factors like blasting, volcanoes, dams, etc. can also cause the occurrence of landslides indirectly.

2.3 Remote Sensing Software-Geographic Information System (GIS) and it's application:

Remote sensing can be defined as the process of obtaining information about a place through the incorporation of photogrammetry as well as satellite imagery based on the radiation emitted or reflected from the features present at that place. This method is widely used by a lot of research scholars across the globe for a lot of applications such as land-use mapping, weather forecasting, environmental study, natural hazards study, and resource exploration. With the advancement of science and the increasing need for remote sensing, the Environmental Systems Research Institute (ESRI) developed a Geographic Information System (GIS) software namely ArcGIS in 1999 for the systematic representation as well as analysis of the remotely sensed data.

In the past few years, GIS software packages were developed for facilitating an enhanced degree of representation and analysis of the remotely sensed data through the application of tools which are developed through the python-based scripts. These tools can be utilized for the application of various mathematical or computational models for the development of new model-based maps.

In this research work, we will focus on the detailed application of tools related to the landslide mapping which were involved in the completion of the project.

For detailed research and analysis of landslides, Remote sensing and GIS-based technologies are becoming hugely popular across the globe. This is because every single step involved in a detailed analysis of landslides can be easily shown in the software:

- Preparation and representation of landslide inventory
- Development of maps from landslide causative factors
- Reclassification and tabulating area for each landslide causative factors
- Landslide zonation map through the application of Frequency ratio and Shannon Entropy models.

- Validation of the produced maps

GIS is widely utilized for generating landslide susceptibility maps for the identification of landslide-prone areas in advance. Various models and approaches can be incorporated within the GIS with the help of other software like Microsoft Excel for generating fairly accurate landslide susceptibility maps (Mezughi et al. 2011).

2.4 Landslide identification and mapping:

The preliminary task in the detailed analysis of landslide susceptibility/ landslide hazard zonation is the preparation of a landslide inventory map which includes the details about the landslides that have occurred in the past in the taken area (Pourghasemi et. al 2012). This is primarily done for the evaluation of the models that can be possibly incorporated for the generation of landslide susceptibility maps in the future and for studying the causative factors responsible for the landslide occurrence (Guzzetti et al, 2012; Regmi et al, 2014; Paliaga et al, 2018). In this project, a total of 200 landslide locations from Chamoli District, Uttarakhand in point shapefile format were taken from the Bhukosh Portal of the Geological Survey of India.

The credibility of the maps produced without any sort of validation will always be questionable. Hence, for establishing the validity of the produced landslide susceptibility maps, we need to divide the dataset containing landslide inventory (Chung and Fabbri, 2003). Out of these 200 points, 20% (40 points) were randomly selected through the geostatistical analyst tool and were taken in the testing dataset whereas the remaining 80% points (160 points) were taken in the training dataset. The training dataset will be used for the preparation of landslide susceptibility maps whereas the testing datasets will be used for the validation of the outputs given by the produced landslide susceptibility maps.

Being the youngest mountain range in the world, the Himalayas are geo-dynamically active and consists of fragile and unstable soil slopes, making the Himalayan ecosystem vulnerable to a number of landslides (Chauhan et al. 2010).

Raman and Punia (2012) stated that nearly 0.49 sq. km or 15% of India’s total area is highly susceptible to landslide occurrence. According to the analysis done by NASA (2019), a

reported number of 6779 individuals lost their lives due to 958 landslide events in India, where Uttarakhand leads the list with 5,226 deaths.

The Indian states of Jammu & Kashmir, Himachal Pradesh and Uttarakhand are a part of the North-Western Himalayan region while the states like Assam, Arunachal Pradesh, Sikkim as well as North Bengal constitute the lower North-eastern Himalayan region. Heavy rainfall (during the monsoon season) is one of the principal reasons causing landslide disasters. Glacial lake outburst flood (GLOF) events, earthquakes, etc. are the other reasons causing landslide occurrence. Moreover, the environmental impacts associated with the developmental projects to accommodate a large population as well as tourists also initiates the occurrence of a landslide event.

Based on the records of the landslide occurrence in an area, the landslide susceptibility maps determine the probability of landslide occurrence in the future in the selected area(s) where similar or identical physical characteristics exist (Westen et al. 2008, Polykretis et al. 2019). For the purpose of landslide susceptibility assessment, many methods have been proposed through the integration of GIS mapping software with various probablisitic as well as machine learning models (Lee et al. 2017).

Sangeeta et al. 2019 studied the pre-and post-earthquake landslide effects after the 1999 Chamoli landslide and prepared landslide susceptibility zonation (LSZ) maps for a part of Chamoli using the Frequency Ratio model using seven controlling factors, i.e., slope angle, slope aspect, slope curvature, geology, distance to drainage, normalized difference vegetation index (NDVI) and peak ground acceleration (PGA) was prepared in Geographic Information System (GIS).

Pathak (2016) carried out a detailed research study around the Chamoli-Joshimath area in the in the Himalayan region and prepared a Landslide susceptibility zonation (LSZ) map of the area. Using a total of seven landslide causative factors, a landslide susceptibility map was substantiated by multiplying the weights of each thematic layer by the ranks of the classes (in raster). The factors namely Geomorphology, Lithology, Slope in Degree, Lineament Density, Drainage Density, Debris Thickness and Proximity to Faults. The most causative/triggering factors received the highest rankings, while the least causative/triggering factors received the

lowest. These rankings were determined using expert knowledge of the taken region gathered through expert field observation.

CHAPTER 3- STUDY AREA

3.1 Uttarakhand:

Uttarakhand is among one of the twelve states along with the Indian Himalayan Region, stretching about 53,483 square kilometers as depicted in Fig 2. It has elevation an elevation range of 187 meters for the lowest point to 7816 meters for the highest point. It is surrounded by four Indian states Himachal Pradesh, Punjab, Haryana and Uttar Pradesh. Additionally, on it's Eastern side, it also shares an international border with China and Nepal.

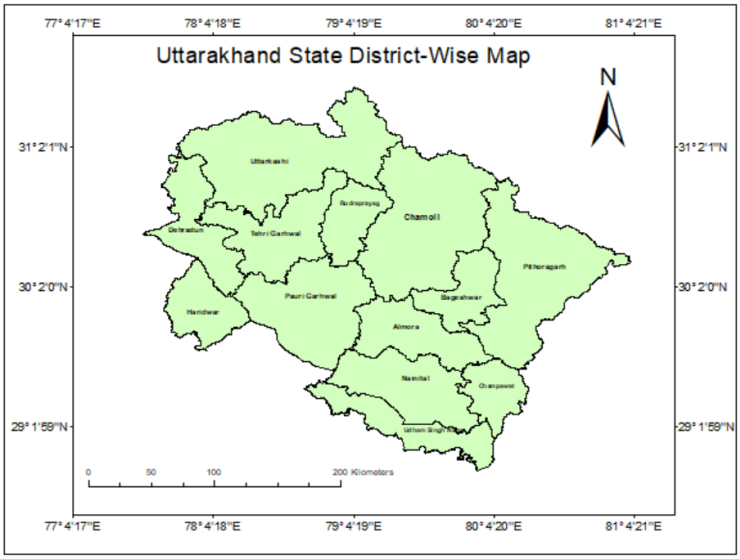

Fig. 3.1 Uttarakhand State map

According to Indian culture and literature, Uttarakhand is the land of the two most holy rivers in India, the Ganga and Yamuna. Both of these two rivers have their origin points situated in Uttarakhand. Other famous rivers in the state include Bhagirathi, Dhauli Ganga, Kali Ganga, Girthi Ganga, Rishi Ganga, Bal Ganga, Bhilangna River, Tons River, Alaknanda, Nandakini, Pindar, Kosi, and Mandakini.

3.2 Chamoli District:

There are a total of 13 districts in Uttarakhand. The area of focus for this study lies in the Chamoli district. This area is a popular tourist place due to several shrines and temples which attract a lot of pilgrimage tourists. Neighboring districts of Chamoli include Uttarkashi in the north-west, Pithoragarh in the south-west, Almora in the south-east, Rudraprayag in the south-west, and Tehri Garhwal in the west. The district's geographical area is around 7520 square kilometres. The entire district consists of a total of twelve tehsils namely: Chamoli, Joshimath, Pokhri, Karanprayag, Gairsain, Tharali, Dewal, Narayanbagar, AdiBadri, Jilasu, Nandprayag and Ghat. Chamoli district also consists of several important rivers and their tributaries. Alaknanda, traversing a distance of 229 km. before it confluence with Bhagirathi at Devprayag and constituting the Ganga is the major river. There are 226 villages in the entire district.

Fig 3.2*: Chamoli district map (Source: Chamoli District Website | India*)

The geology of the region shows that the Himalayas are the young mountains in the world. The landmass which is presently occupied by the Himalayas was occupied by the great Tethys Sea during early Mesozoic times or the secondary geological period.

Geologists estimate that the formation of the Himalayan mountains took place during the end of the Mesozoic period. However, the history behind their actual structure has just started to unravel as with the present tools and equipment, the dating of some rocks is not yet possible. A significant uplift has been seen in some parts of the area since the mid-Pleistocene period, in others, there are great stretches of high but subdued topography and elsewhere there are the deepest gorges.

The mountain masses present in this area generally span from North to South. The district has geological features which give rise to two major divisions which lie North and South of an imaginary line that extends from East-South East between the villages of Hilang in Joshimath and Loharkhet in the adjoining District of Pithoragarh. The peaks have a higher elevation that is covered with snow consisting of medium to high-grade metamorphic rocks and are intruded by later volcanic rocks that form the Northern Division.

The Southern division is made up of lower-altitude mountain ranges with sedimentary and low-grade metamorphic rock formations intruded by later volcanic materials. The first division comprises rock formations such as quartzites, marbles, and various forms of micaceous schists and gneisses with intermittent occurrences of garnet, graphite, iron, kynite, mica, and vein quartz, according to the pieces of information available the geologists. Geologists have much more knowledge about the division that exists on the southern side of the imaginary line and it consists of rocks such as gneisses, limestone, phyllites, quartzite, and sericite-biotite schists and slates.

CHAPTER 4-METHODOLOGY AND DATABASE PREPARATION

4.1 Methodology adopted:

This research study involves systematic and detailed steps in the methodology where two statistical models namely Frequency Ratio (FR) and Shannon Entropy (SE) produce landslide susceptibility maps in part of the Chamoli district using the landslide inventory data collected through remote sensing techniques as shown below in figure 4.1. The landslide inventory contains information about the landslide occurrences that have previously occurred in the area.

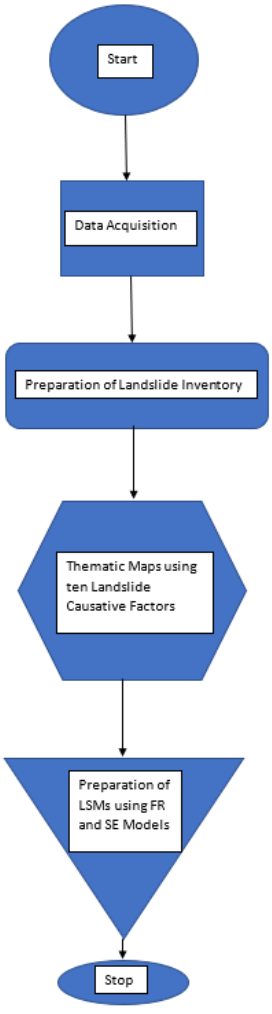

Figure 4.1 Flow Chart of the methods involved

Preparing a landslide inventory map of the area for proceeding with such studies related to landslide susceptibility mapping is the first yet crucial task. Any study dealing with landslide susceptibility mapping is incomplete without accounting for the landslide causative factors which affect the landslide occurrence in an area. In this study, a total of ten such landslide causative factors were considered based on the literature review.

The adopted landslide susceptibility evaluation procedure can be classified as:

a) Selection of landslide-inducing factors for the area
b) Generation of thematic layers for the chosen factors
c) Preparation of a new landslide incidence map
d) Compilation of newly mapped and historical landslide data
e) Application of the bi-variate probabilistic FR and SE methods to calculate ratios for every factor class and factor maps.
f) Landslide Susceptibility Maps (LSM) creation and classification
g) Model validation and comparison through:
    i. Area Under Curve (AUC) of ROC

4.2 Data used:

The data for the advancement of this research study was first collected from various sources, and then the district's required area, as well as the landslide causative factors, were mapped on GIS system software ArcMap. A total of ten landslide causative factors were considered in this research study namely: elevation, slope, aspect, curvature, lithology, distance to roads, distance to faults/lineaments, distance to rivers, and topographic wetness index, and stream power index.

Table 4.1 Data used and their various sources

DATA USED	DATA SOURCE
Digital Elevation Model	Open Topography: SRTM GLI Global, resolution: 30m.
Lithology, Roads, Lineament, Rivers, Landslide Points	Bhukosh Portal, Geological Survey of India.
India Districts Shapefile	Advances in Geographical Research

The Digital Elevation Model (DEM) was acquired from SRTM GL1 data available on an open-source Open Topography portal having a spatial resolution of 30m. The obtained DEM was used to obtain various factors maps such as slope, aspect, curvature and elevation. These factors can be utilized as the landslide causative factors as they affect the landslide occurrence directly or indirectly. These factors will also be used for the preparation of thematic maps which will be shown in the subsequent sections. As the mapping needs to be done for the DEM, the coordinate system for the DEM was changed from the geographic coordinate system to the projected coordinate system namely World Geodetic System 1984 in Universal Transverse Mercator zone 43N.

4.3 Derivatives obtained from DEM:

In this research study, various factors were obtained from DEM namely slope, aspect, curvature, TWI and SPI. All of them were extracted for the taken study area of Chamoli district.

4.3.1 Slope

With the increase in the slope angle, even a sufficiently thick soil becomes more unstable (Nohani et al. 2019). Due to this, a rise in the slope angle generally corresponds to a higher likeliness of landslide occurrence. The slope map was obtained from DEM through the utilization of the "Spatial Analyst" tool in ArcGIS. The values of slope angles for the study area were divided into five classes namely 0-16º, 16º -27º.14º, 27.14º -37.24º, 37.24º -48.91º, and greater than 48.91º.

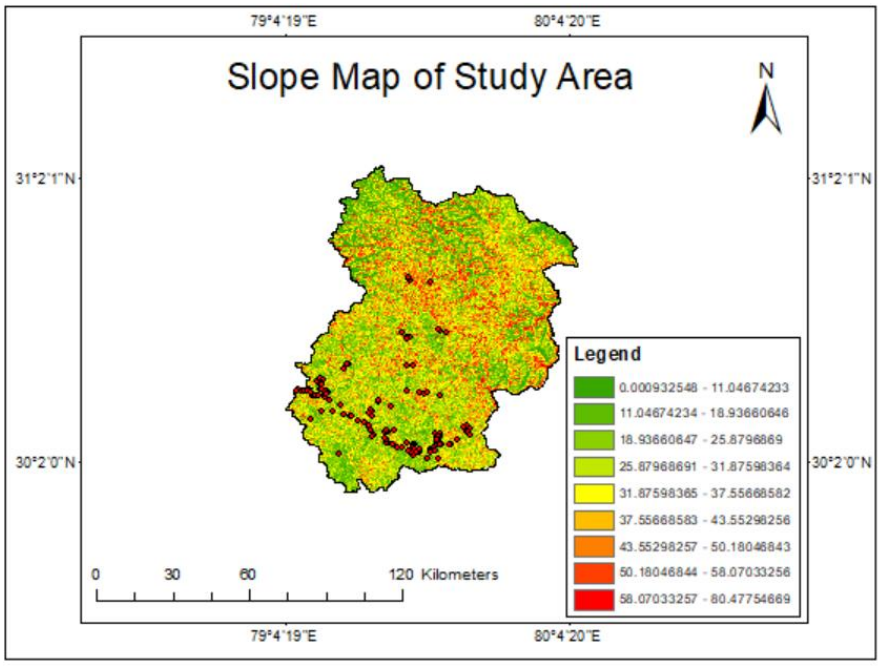

Fig. 4.2 Slope map

4.3.2 Aspect

Through effective utilization of the spatial analyst tool in ArcGIS, the aspect map showing the directions of the slope in the area was prepared. The classification done by the GIS software for the aspect is classified as North at 0° back to North at 360°. However, for the flat surfaces, there is no aspect and it's value is taken as (-1) by the software and is denoted by grey cells in the aspect map.

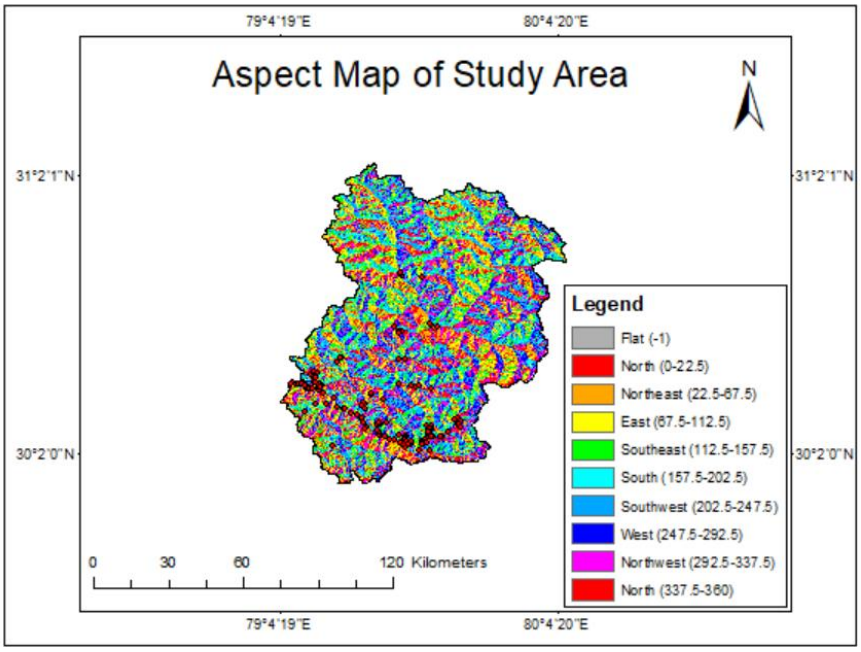

Fig. 4.3 Aspect map

4.3.3 Curvature

The curvature map was also derived from DEM through the incorporation of a spatial analyst tool in ArcGIS software. The value of curvature represents the shape or curvature of the slope of the drainage basin through which, the runoff or erosion can be easily shown comprehensively (Rejith et al. 2019).

The curvature map thus generated has values of the classes where the negative values represent convex surfaces whereas the positive values represent the concave surfaces. Moreover, the values corresponding to 0 or nearly equal to zero represent linear surfaces or no curvature. The detailed curvature map is shown in figure 4.4.

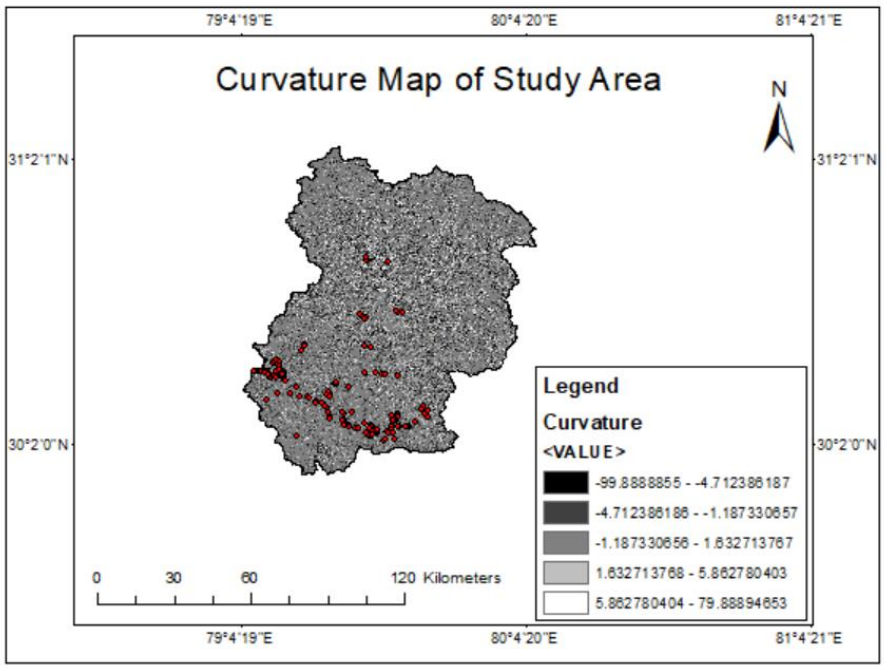

Fig. 4.4 Curvature map

4.3.4 Elevation

The elevation map can be directly obtained from DEM and then it was clipped for the study area. The elevation map was divided into a total of five classes where the elevation ranges from 654.84 m-7777.55 m as shown in figure 4.5.

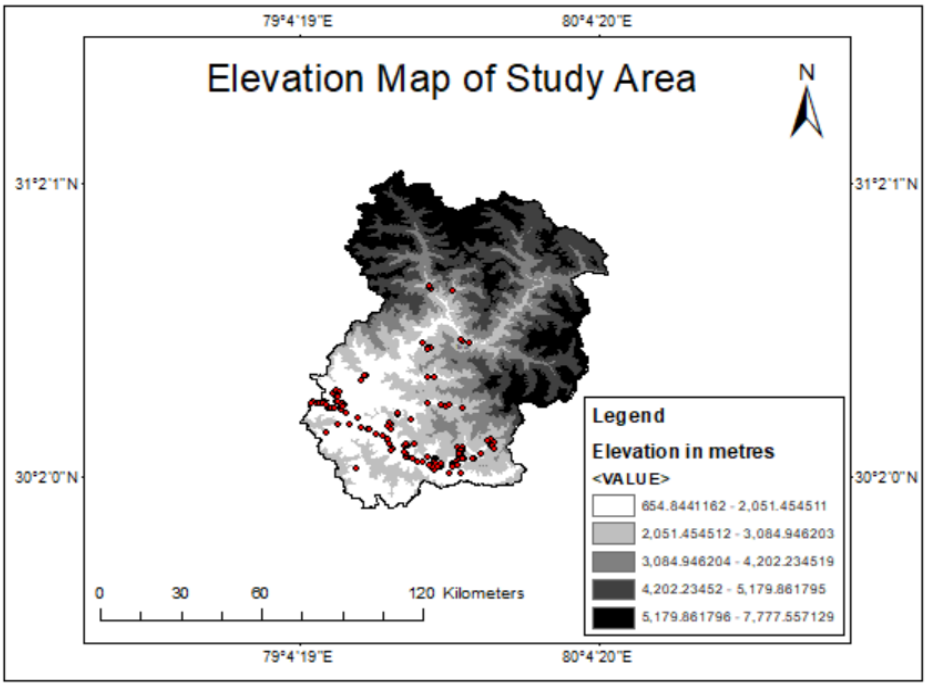

Fig. 4.5 Elevation map

Elevation does not affect the landslide occurrence directly. However, the human settlement, as well as infrastructural development projects, are more segregated at the lower elevation which directly affects the landslide occurrence.

4.3.5 Topographic Wetness Index

The topographic wetness index (TWI) is another factor that influences an area's landslide susceptibility. It is a derivative of DEM. TWI considers the area which contributes to the upslope area and computes the flow and accumulation of the water along with the steady-state wetness present in the taken area (Pourghasemi et al. 2013a). Numerically, TWI is calculated as:

TWI= Ln (Flow Accumulation+0.001)/ (Slope in Percentage/100+0.001)

A TWI value less than 5 indicates a low TWI value whereas a TWI value greater than 10 indicates a higher TWI value. TWI values ranging from 5 to 10 correspond to an intermediate TWI. The TWI map made by ArcMap classifies TWI values in five ranges where the maximum part lies in the range of -5077 to 82.105 as shown in figure 4.6.

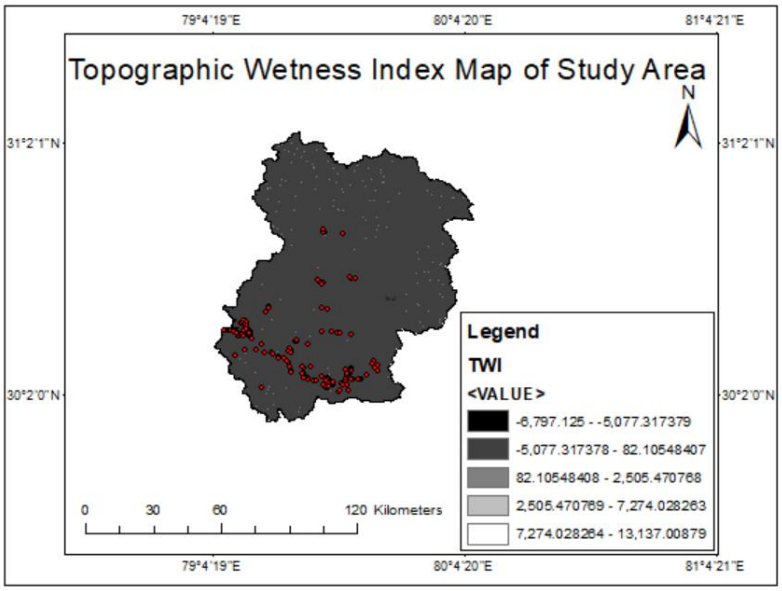

Fig 4.6 Topographic Wetness Index (TWI) map

4.3.6 Stream Power Index:

Another DEM derivative is the stream power index (SPI), which quantifies the stream's potential to alter the geomorphology of an area via gully erosion and transportation.SPI co-relates the ability of the flowing water to cause erosion through discharge and catchment areas (Chen and Yu 2011; Pourghasemi et al. 2013b). The areas where the overland water has a higher potential to cause erosion are highlighted by SPI (Wilson and Gallant 2000). Therefore, SPI adversely affects the landslide susceptibility of an area. Numerically, SPI can be calculated as:

SPI= Ln (Flow Accumulation+0.001) * ((Slope in Percentage/100)+0.001))

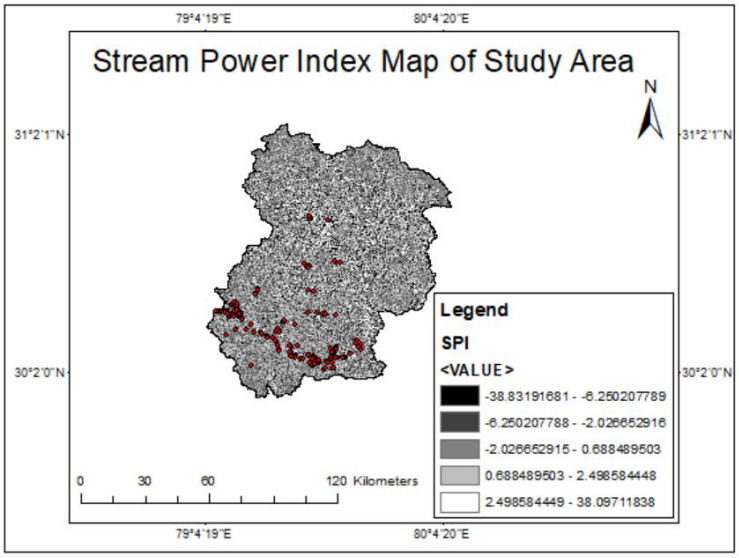

Fig 4.7 Stream Power Index (SPI) map

The SPI map generated by ArcMap classifies the range of SPI within five classes ranging from -38.83 to 38.09 as shown in figure 4.6.

4.4 Other prepared thematic layers

The following thematic layers were extracted using data from other sources. They were also chosen to evaluate their relationship to slope instability in the region.

4.4.1 Distance to roads

There are numerous road construction and widening projects which have been constructed in Uttarakhand throughout the past years. In the study area, which lies in the Chamoli district, has also become more susceptible to landslides due to such projects. To calculate distances to roads, firsty the road data was downloaded road in shapefile format from the Geological Survey of India's Bhukosh portal and was converted into a projected coordinate system namely WGS 1984 UTM Zone 43N as mentioned earlier, within the ArcMap. Then, through the Euclidean Distance tool, the distance to roads will be calculated by the software and it will be resampled to 30m resolution raster. It must be noted that the Euclidean distance tool will automatically convert the shapefile data into raster format.

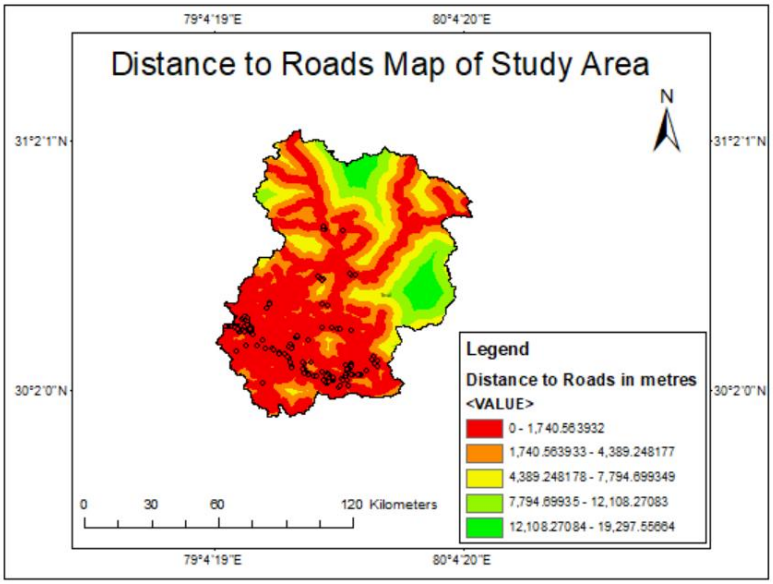

Fig. 4.8 Distance to road map

The distance to road in the prepared map was classified into five categories ranging from 0 – 19297 m as in Figure 4.7.

4.4.2 Distance to faults/lineaments

Presence of faults or lineament again, increase the likelihood of landslide occurrence as the region becomes more susceptible to earthquake, which causes vibrations and in turn, initiates the erosion or movement of soil. In this study, the lineament data was obtained from Bhukosh portal of Geological Survey of India and the calculation of distance to lineament was done in an exact similar way as that of the "Distance to roads" through Euclidean Distance tool of the ArcMap after converting it's the coordinate system to WGS 1984 UTM Zone 43N and converting the final output into 30 m raster resolution. The obtained map for distance to river consists of a total of five classes of distance range ranging from 0-52042.81 m.

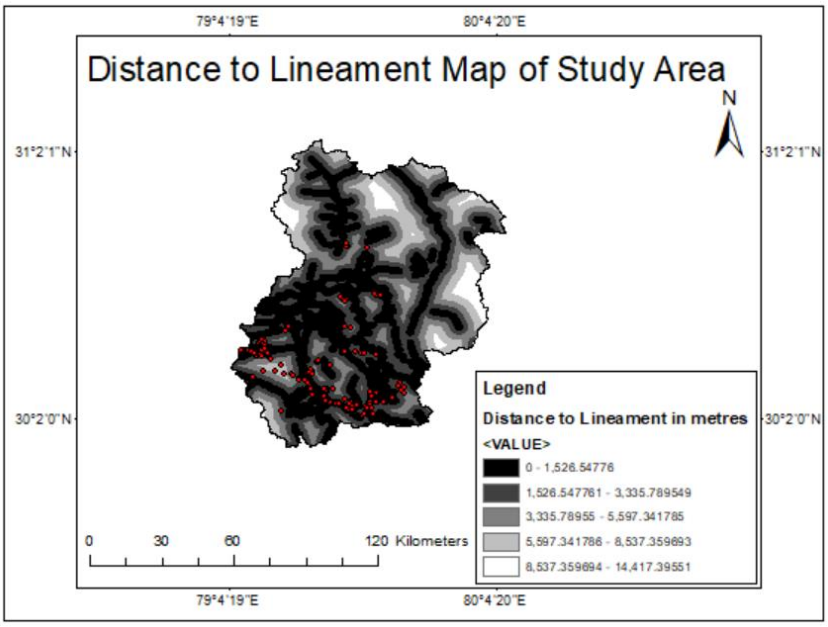

Fig. 4.9 Distance to faults/lineaments map

4.4.3 Lithology

Generally, lithology comes out to be one of the most important landlide causative factor (Lee and Pradhan 2006; Kamp et al. 2008; Shahabi et al. 2014; Zhu et al. 2014; Meinhardt et al. 2015; Myronidis et al. 2016; Zhang et al. 2016; Autade and Pardeshi 2017). The data for lithology of the area was obtained from Bhukosh Portal of Geological Survey of India in shapefile format and then rasterized and also, resampled into a raster of 30 m raster resolution after converting the co-ordinate system to WGS 1984 UTM Zone 43N. Lithology map of the area reveals that a total of 48 lithologic formations exist in the area as shown in Figure 4.9.

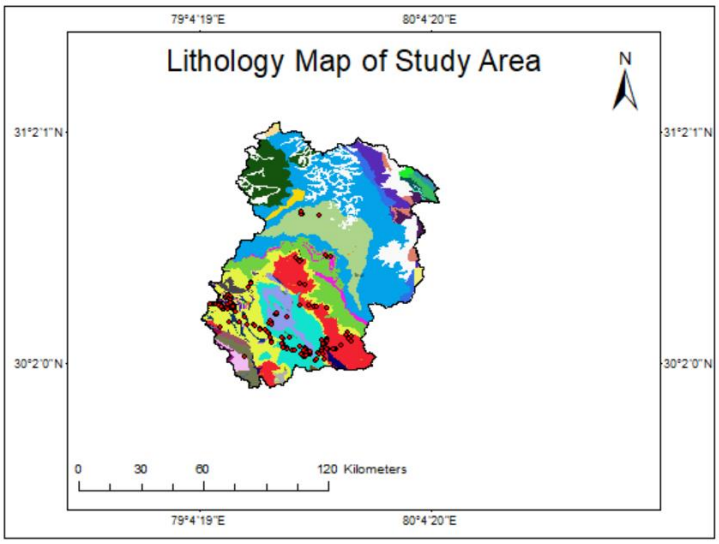

Figure 4.10 Lithology Map

Figure 4.10 Continued

4.4.4 Distance to River

River flow can destabilize a slope by bringing it into flowing condition which may initiate a landslide. Therefore, the larger will be the distance from the river, the safer will be the slope. The data required for mapping this landslide causative factor was obtained from Bhukosh portal of Geological Survey of India and the calculation of distance to river was done in an exact similar way as that of the "Distance to roads" and "Distance to lineament" through Euclidean Distance tool of the ArcMap after converting the coordinate system of the obtained data to WGS 1984 UTM Zone 43N and converting the final output into 30 m raster resolution.

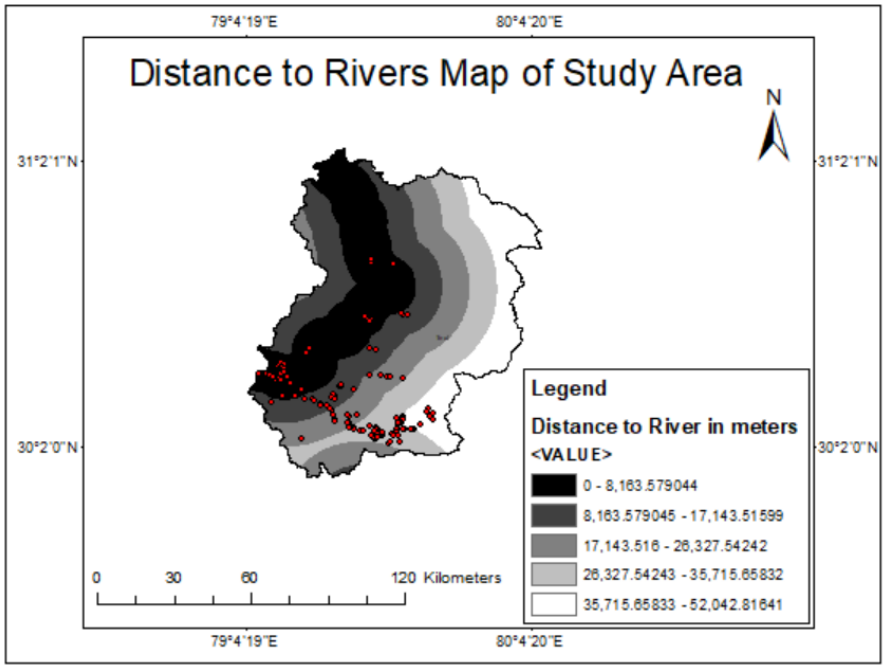

Figure 4.11 Distance to river map

4.5 Landslide Inventory map

As discussed earlier, landslide inventory map is the first step for the preparation of landslide susceptibility map of an area. A landslide inventory was manifested from the necessary data about prior landslides that occurred in the taken area. A higher number of landslide inventory gives us more accurate results of the prediction models. Here, the landslide inventory was

acquired from Bhukosh portal of the Geological Survey of India in point shapefile format and 200 landslide points were chosen for the purpose of landslide susceptibility mapping.

4.5.1 Random splitting of samples

The taken points were randomly split into two sets namely training and testing datasets. The training dataset was used for the generation of landslide susceptibility maps whereas the testing dataset was used for the validation/testing purpose. The splitting of points can be done easily through the "Geostatistical Analyst" tool in GIS. Out of the taken 200 points in landslide inventory, 80% of the points were taken in the training dataset whereas the remaining 20% were taken in the testing dataset.

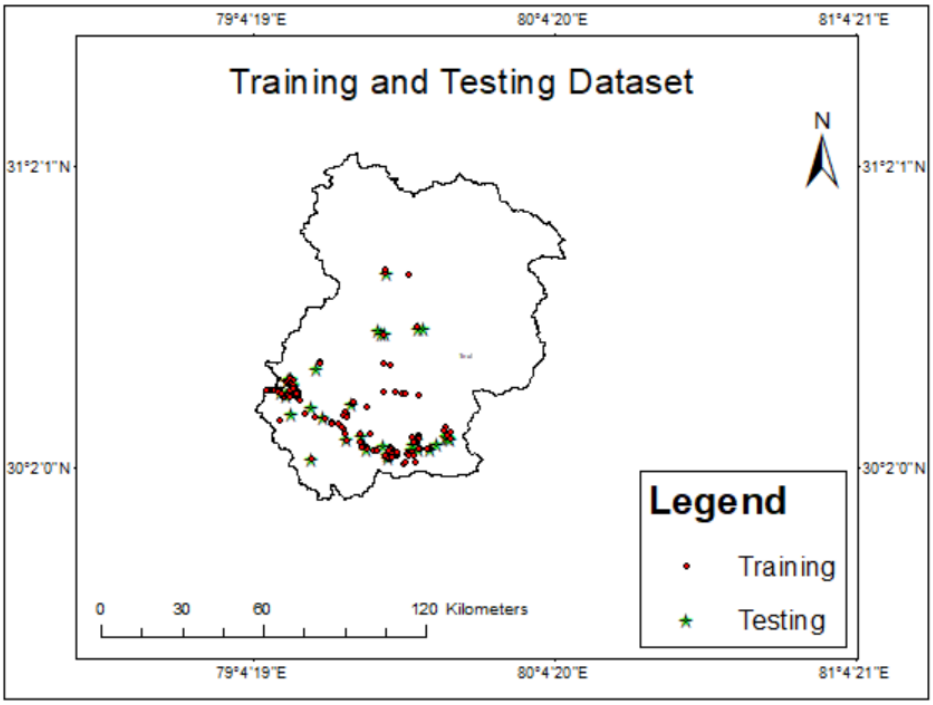

Figure 4.12 Training and Testing Dataset

CHAPTER 5- ADOPTED PROBABILITY APPROACHES: CONCEPTS AND COMPUTATION RESULTS

5.1 Statistical methods incorporated in the study:

Probabilistic statistical models can be of two types namely Bivariate models and multivariate models. Bivariate models rely on the relationship within the parameters and compute the results whereas the computation of results in the multivariate models is done through an additional relative weight determination between the factors. However, the weights allocated for each factor do not rely on the knowledge of experts, they are not widely used due to their subjective application.

In this study, two statistical bivariate models were used for the determination of landslide susceptibility namely Frequency ratio and Shannon Entropy.

5.1.1 Frequency Ratio (FR):

The frequency ratio (FR) method is a simple yet reliable technique for performing landslide susceptibility mapping on a wide scale of applications (Choi et al. 2012; Ehret et al. 2010; Lee 2014; Lee and Pradhan 2006; Mezughi et al. 2011; Mohammady et al. 2012; Yalcin et al. 2011; Yilmaz 2009). This bivariate statistical technique works well with GIS-based ArcMap software (Lee 2014; Yilmaz and Keskin 2009; Yalcin et al. 2011).

FR was firstly calculated for each class of each factor using Microsoft Excel and then, the corresponding relative frequencies along with the prediction rate for each factor was computed. Individual factor classes were then reclassified by changing their existing values by the relative frequency (RF) values. Then, individual prediction rates (RF) will be multiplied with the reclassified factor classes through the “Raster Calculator” tool in ArcMap through which, the landslide susceptibility map for the study area will be generated.

The FR as well as RF values for each class of each causative factor were computed using Equation 5.1.

$$FR = \frac{\%\ Landslide\ Pixels}{\%\ Class\ Pixels} \quad (5.1)$$

$$RF = \frac{FR}{Total\ sum\ of\ Frequency\ Ratios\ for\ that\ causative\ factor} \quad (5.2)$$

The prediction rate for each causative factor can be calculated in excel as:

$$PR = \frac{RFmax - RFmin}{(RFmax - RFmin)min} \quad (5.3)$$

After the reclassification of each factor class in GIS after replacing their existing values with their respective relative frequencies, the landslide susceptibility map for the area can be generated through the raster calculator in GIS by using following expression:

$LSM=(PR_{slope}*Slope)+(PR_{aspect}*Aspect)+(PR_{elevation}*Elevation)+(PR_{lithology}*Lithology)+(PR_{twi}*TWI)+(PR_{spi}*SPI)+(PR_{distance\ to\ roads}*Distance\ to\ roads)+(PR_{distance\ to\ lineament}*Distance\ to\ lineament)+(PR_{distance\ to\ river}*Distance\ to\ river)+(PR_{curvature}*Curvature)$…….(5.4)

5.1.2 Shannon Entropy (SE):

Entropy shows randomness or disorderness in a continuous probability distribution data set. Basically, it is used to represent the instability or uncertainty in a given data set in natural phenomena (Shannon, 1948). In this method, individual weights for each landslide causative factor are calculated and those calculated weights will be multiplied with each causative factor in GIS through the raster calculator tool.

Numerically, it can be easily visualized as an extension of the FR method because the weight calculation for each factor is based on RF values calculated for the FR method. Here, the weights are always multiplied with the reclassified landslide causative factors based on RF.

For the calculation of weights for each landslide causative factor, the following equations are used:

$$E = -K \sum RF * Log(RF) \quad (5.5)$$

Here, $K = \frac{1}{Log(M)}$, E= Entropy

Where, M= Number of classes in each landslide causative factor

Now, the individual weight for each factor can be calculated through the following equation:

$$Wi = \frac{1 - E}{\sum(1 - E)} \quad (5.6)$$

Now, the landslide susceptibility map (LSM) for the taken study area can be computed by multiplying each landslide causative factor with their corresponding calculated weights through Shannon Entropy technique as shown in the following equation:

LSM=(W_{slope}*Slope)+(W_{aspect}*Aspect)+($W_{elevation}$*Elevation)+($W_{lithology}$* Lithology)+(W_{twi}*TWI)+(W_{spi}*SPI)+($W_{distance\ to\ lineament}$*Distance to lineament)+($W_{distance\ to\ roads}$* Distance to roads)+($W_{distance\ to\ rivers}$*Distance to rivers)+($W_{curvature}$*Curvature)……(5.7)

5.2 Computation results:

The computation of weight values for every class of every factor map gives an insight into the landslide distribution and about the degree of correlation of each class to landslide occurrences. The results from the Frequency Ratio (FR), Shannon Entropy (SE)

Table 5.1 Frequency Ratio (FR) Results for each landslide causative factor

Factor	Factor Classes	Landslide Pixels	% landslide pixels	Class Pixels	% Class pixels	Frequency Ratio	RF
	0-16.096	4500	3.14	1364701	15.70	0.20	0.04
SLOPE IN DEGREES	16.096-27.142	28800	20.13	2180102	25.08	0.80	0.18
	27.142-37.241	55800	38.99	2483989	28.58	1.36	0.30
	37.241-48.918	45000	31.45	1861709	21.42	1.47	0.33
	48.918-80.477	9000	6.29	802298	9.23	0.68	0.15
	Total	143100	100.00	8692799	100.00	4.52	1.00
	Flat	13500	9.43	837549	9.63	0.98	0.10
ASPECT	North	15300	10.69	899922	10.35	1.03	0.10
	North-East	8100	5.66	862238	9.92	0.57	0.06
	East	12600	8.81	925760	10.65	0.83	0.08
	South-East	14400	10.06	870578	10.01	1.00	0.10
	South	18900	13.21	875035	10.07	1.31	0.13
	South-West	27900	19.50	939160	10.80	1.80	0.18
	West	8100	5.66	827940	9.52	0.59	0.06
	North-West	9900	6.92	816554	9.39	0.74	0.07
	North	14400	10.06	838063	9.64	1.04	0.11
	Total	143100	100.00	8692799	100.00	9.91	1.00

Factor	Factor Classes	Number of points	% of points	Class Area	% Class area	Frequency Ratio	RF
	(-99.888)-(-5.107)	1800	1.26	250797	2.88	0.44	0.10
CURVATURE	(-5.107)-(-1.330)	27000	18.87	1583929	18.19	1.04	0.24
	-1.330-1.225	88200	61.64	5049936	57.99	1.06	0.25
	1.225-5.114	22500	15.72	1576960	18.11	0.87	0.20
	5.114-79.888	3600	2.52	247149	2.84	0.89	0.21
	Total	143100	100.00	8708771	100.00	4.29	1.00

Factor	Factor Classes	Number of points	% of points	Class Area	% class area	Frequency Ratio	RF
	AMPHIBOLITE	0	0.00	22652	0.26	0.00	0.00
LITHOLOGY	AMPHIBOLITE AND META-NORITE	0	0.00	207657	2.38	0.00	0.00
	BASAL CONGLOMERATE AND MASSIVE QUARTZITE	900	0.63	31039	0.36	1.76	0.02
	BASIC META-VOLCANICS	25200	17.61	726389	8.34	2.11	0.02
	BASIC ROCK	0	0.00	506652	5.82	0.00	0.00
	BIOTITE, HORNBLENDE GRANITE	34200	23.90	913150	10.49	2.28	0.02
	CALC SILICATE, QUARTZITE, SCHIST, MARBLE BAND	0	0.00	1089	0.01	0.00	0.00
	CARB. SHALE, SILTSTONE, SANDSTONE WITH NODULES	34200	23.90	569413	6.54	3.66	0.03
	CARBONACEOUS PHYLLITE, QUARTZITE AND SCHIST	6300	4.40	69853	0.80	5.49	0.05
	CHLORITE SCHIST, HORNBLENDE-ALBITE-ZOISITE SCHIST	14400	10.06	20560	0.24	42.62	0.37
	EPIDIORITE	0	0.00	2E+06	22.89	0.00	0.00
	GAR. MICA & CHLORITE SCHIST, QTZ WITH PHYLLITE	0	0.00	4622	0.05	0.00	0.00
	GLAUCONITIC SANDSTONE, SHALE WITH SILTSTONE BANDS	2700	1.89	19372	0.22	8.48	0.07
	GNEISS, KYANITE SCHIST, QUARTZITE, CALC SILICATE	0	0.00	28985	0.33	0.00	0.00
	GRANITE	0	0.00	106411	1.22	0.00	0.00
	GRANITE GNEISS WITH RAFTS OF QUARTZITE, SCHIST	2700	1.89	802398	9.21	0.20	0.00
	GRANITE, GNEISS AND SCHIST	900	0.63	576540	6.62	0.09	0.00
	GRANULITE, GARNET MICA SCHIST, FELSPATHIC SCHIST	0	0.00	50452	0.58	0.00	0.00
	GRAVEL, PEBBLE, SAND, SILT AND CLAY	0	0.00	11474	0.13	0.00	0.00
	GREY NODULAR LIMESTONE & FOSSILIFEROUS LIMESTONE	4500	3.14	7454	0.09	36.74	0.32
	GREY SAND, SILT AND CLAY	900	0.63	15506	0.18	3.53	0.03
	LIMESTONE WITH SHALE	0	0.00	1503	0.02	0.00	0.00
	LIMESTONE, DOLOMITE, SHALE, CARB. PHYLLITE/SLATE	0	0.00	6812	0.08	0.00	0.00
	LIMESTONE, SILTSTONE, MARL AND SHALE	12600	8.81	257839	2.96	2.97	0.03
	MEDIUM TO COARSE GRAINED BIOTITE GRANITE	0	0.00	153713	1.77	0.00	0.00
	META BASICS SILLS AND DYKES	0	0.00	9699	0.11	0.00	0.00

	MIGMATITE GNEISS WITH MARBLE BANDS	0	0.00	14587	0.17	0.00	0.00
	ORTHOQUARTZITE WITH SHALE BANDS	0	0.00	4649	0.05	0.00	0.00
	PHYLLITE WITH CHLORITIC, GRAPHITIC & CARBONACEOUS	0	0.00	35225	0.40	0.00	0.00
	PHYLLITE, QTZ, SHALE, DOLOMITE, TUFF WITH DOLERITE	0	0.00	189	0.00	0.00	0.00
	PORPHYRITIC NONFOLIATED GRANITE	0	0.00	27540	0.32	0.00	0.00
	QUARTZ-SERICITE-CHLORITE SCHIST & LIMESTONE	0	0.00	55043	0.63	0.00	0.00
	QUARTZITE AND QUARTZ MICA SCHIST	0	0.00	5879	0.07	0.00	0.00
	QUARTZITE AND SLATE WITH BASIC METAVOLCANICS	0	0.00	139167	1.60	0.00	0.00
	QUARTZITE WITH HORNBLENDE-ALBITE-ZOISITE SCHIST	0	0.00	24909	0.29	0.00	0.00
	QUARTZITE, GARNETIFEROUS SCHIST AND PARAGNEISS	1800	1.26	42672	0.49	2.57	0.02
	QUARTZITE, SHALE, PHYLLITE AND CONGLOMERATE	0	0.00	71722	0.82	0.00	0.00
	QUARTZITE, SLATE, LENSOIDAL LIMESTONE AND TUFF	0	0.00	80547	0.92	0.00	0.00
	SCHIST, GNEISS, MARBLE AND BASIC INTRUSIVES	0	0.00	33159	0.38	0.00	0.00
	SCHIST, AUGEN GNEISS, QUARTZITE & AMPHIBOLITE	0	0.00	1988	0.02	0.00	0.00
	SCHISTOSE GRIT, SLATE, QUARTZITE WITH VOLCANICS	0	0.00	60060	0.69	0.00	0.00
	SERICITE QUARTZ SCHIST, CHLORITE SCHIST	0	0.00	4139	0.05	0.00	0.00
	SHALE WITH SHALY LIMESTONE	0	0.00	2546	0.03	0.00	0.00
	SHALE, QUARTZITE WITH CALCAREOUS NODULES	0	0.00	2923	0.03	0.00	0.00
	SILTSTONE, SHALE, LIMESTONE & CALCAREOUS SANDSTONE	0	0.00	901419	10.35	0.00	0.00
	SLATE, CARB. SHALE, QUARTZITE, SILTSTONE, PHYLLITE	1800	1.26	75368	0.87	1.45	0.01
	SLATE, CARBO. SHALE, QUARTZITE, SILTSTONE PHYLLITE	0	0.00	9269	0.11	0.00	0.00
	UNMAPPED	0	0.00	1119	0.01	0.00	0.00
	Total	143100	100.00	8708289	100.00	113.97	1.00

Factor	Factor Classes	Number of points	% of points	Class Area	% class area	Frequency Ratio	RF
	0-1526.547	82800	57.86	3355509	38.53	1.50	0.48
DISTANCE TO LINEAMENT (m)	1526.547-3335.789	54900	38.36	2477447	28.45	1.35	0.43
	3335.789-5597.341	3600	2.52	1541854	17.70	0.14	0.05
	5597.341-8537.359	1800	1.26	984131	11.30	0.11	0.04
	8537.359-14417.395	0	0.00	349831	4.02	0.00	0.00
	TOTAL	143100	100.00	8708772	100.00	3.10	1.00

Factor	Factor Classes	Number of points	% of points	Class Area	% class area	Frequency Ratio	RF
	0-1740.563	141300	98.74	4356108	50.02	1.97	0.97
DISTANCE TO ROAD (in m)	1740.563-4389.248	1800	1.26	2007799	23.05	0.05	0.03
	4389.248-7794.699	0	0.00	1189357	13.66	0.00	0.00
	7794.699-12108.270	0	0.00	763012	8.76	0.00	0.00
	12108.270-19297.556	0	0.00	392590	4.51	0.00	0.00
	TOTAL	143100	100.00	8708866	100.00	2.03	1.00

Factor	Factor Classes	Number of points	% of points	Class Area	% class area	Frequency Ratio	RF
	0-8163.579	48600	33.96	2183475	25.07	1.35	0.28
DISTANCE TO RIVER (in m)	8163.579-17143.515	18000	12.58	2006681	23.04	0.55	0.11
	17143.515-26327.542	18000	12.58	1694265	19.45	0.65	0.13
	26327.542-35715.658	41400	28.93	1563608	17.95	1.61	0.33
	35715.658-52042.816	14400	10.06	1260721	14.48	0.70	0.14
	TOTAL	140400	98.11	8708750	100.00	4.85	1.00

Factor	Factor Classes	Number of points	% of points	Class Area	% class area	Frequency Ratio	RF
	(-38.831)-(-6.250)	5400	3.77	382078	4.40	0.86	0.19
STREAM POWER INDEX	(-6.250-(-2.026)	18000	12.58	1406132	16.18	0.78	0.17
	(-2.026)-0.688	40500	28.30	3206838	36.89	0.77	0.17
	0.688-2.498	69300	48.43	2940930	33.83	1.43	0.31
	2.498-38.097	9900	6.92	756821	8.71	0.79	0.17
	TOTAL	143100	100.00	8692799	100.00	4.63	1.00

Factor	Factor Classes	Number of points	% of points	Class Area	% class area	Frequency Ratio	RF
	(-6797.125)-(-5077.317)	0	0.00	143	0.00	0.00	0.00
TOPOGRAPHIC WETNESS INDEX	(-5077.317)-(82.105)	143100	100.00	8640891	99.40	1.01	1.00
	82.105-2505.470	0	0.00	51652	0.59	0.00	0.00
	2505.470-7274.028	0	0.00	63	0.00	0.00	0.00
	7274.028-13137.008	0	0.00	50	0.00	0.00	0.00
	TOTAL	143100	100.00	8692799	100.00	1.01	1.00

Factor	Factor Classes	Number of points	% of points	Class Area	% class area	Frequency Ratio	RF
	654.844-2023.672	121500	84.91	1757348	20.18	4.21	0.85
ELEVATION (in m)	2023.672-3025.136	21600	15.09	1783202	20.48	0.74	0.15
	3025.136-4122.267	0	0.00	1409342	16.18	0.00	0.00
	4122.267-5127.360	0	0.00	1996202	22.92	0.00	0.00
	5127.360-7777.557	0	0.00	1762677	20.24	0.00	0.00
	TOTAL	143100	100.00	8708771	100.00	4.94	1.00

Table 5.2: Prediction Rate for each landslide causative factor

Feature	**PR**
Aspect	1
Stream Power Index	1.2
Curvature	1.22
Distance From River	1.83
Slope	2.25
Lithology	3.12
Distance From Lineament	4.03
Elevation	7.09
Distance From Road	8.11
Topographic Wetness Index	8.33

Table 5.3 Results of Shannon Entropy

Factor	Factor Classes	Number of points	% of points	Class Area	% class area	Frequency Ratio	RF	RF*LogRF	Ej	1-Ej
	0-16.096	4500	3.14	1364701	15.70	0.20	0.04	-0.06		
SLOPE IN DEGREES	16.096-27.142	28800	20.13	2180102	25.08	0.80	0.18	-0.13		
	27.142-37.241	55800	38.99	2483989	28.58	1.36	0.30	-0.16	0.91	0.09
	37.241-48.918	45000	31.45	1861709	21.42	1.47	0.33	-0.16		
	48.918-80.477	9000	6.29	802298	9.23	0.68	0.15	-0.12		
	TOTAL	143100	100.00	8692799	100.00	4.52	1.00	-0.63		

m	k	Ej
5.00	1.43	0.91

Factor	Factor Classes	Number of points	% of points	Class Area	% class area	Frequency Ratio	RF	RF*logRF	Ej	1-Ej
	Flat	13500	9.43	837549	9.63	0.98	0.10	-0.10		
ASPECT	North	15300	10.69	899922	10.35	1.03	0.10	-0.10		
	North-East	8100	5.66	862238	9.92	0.57	0.06	-0.07		
	East	12600	8.81	925760	10.65	0.83	0.08	-0.09		
	South-East	14400	10.06	870578	10.01	1.00	0.10	-0.10	0.98	0.02
	South	18900	13.21	875035	10.07	1.31	0.13	-0.12		
	South-West	27900	19.50	939160	10.80	1.80	0.18	-0.13		
	West	8100	5.66	827940	9.52	0.59	0.06	-0.07		
	North-West	9900	6.92	816554	9.39	0.74	0.07	-0.08		
	North	14400	10.06	838063	9.64	1.04	0.11	-0.10		
	Total	143100	100.00	8692799	100.00	9.91	1.00	-0.98		

m	k	Ej
10.00	1.00	0.98

Factor	Factor Classes	Number of points	% of points	Class Area	% class area	Frequency Ratio	RF	RF*logRF	Ej	1-Ej
	(-99.88)-(-5.107)	1800	1.26	250797	2.88	0.44	0.10	-0.10		
CURVATURE	(-5.107)-(-1.330)	27000	18.87	1583929	18.19	1.04	0.24	-0.15		
	(-1.330)-(1.225)	88200	61.64	5049936	57.99	1.06	0.25	-0.15	0.98	0.02
	1.225-5.114	22500	15.72	1576960	18.11	0.87	0.20	-0.14		
	5.114-79.888	3600	2.52	247149	2.84	0.89	0.21	-0.14		
	TOTAL	143100	100.00	8708771	100.00	4.29	1.00	-0.68		

m	k	Ej
5.00	1.43	0.98

Factor	Factor Classes	Number of points	% of points	Class Area	% class area	Frequency Ratio	RF	RF*logRF	Ej	1-Ej
	0-1526.547	82800	57.86	3355509	38.53	1.50	0.48	-0.15		
DISTANCE FROM LINEAMENT (in m)	1526.547-3335.789	54900	38.36	2477447	28.45	1.35	0.43	-0.16		
	3335.789-5597.341	3600	2.52	1541854	17.70	0.14	0.05	-0.06	0.60	0.40
	5597.341-8537.359	1800	1.26	984131	11.30	0.11	0.04	-0.05		
	8537.359-14417.395	0	0.00	349831	4.02	0.00	0.00	0.00		
	TOTAL	143100	100.00	8708772	100.00	3.10	1.00	-0.42		

m	k	Ej
5.00	1.43	0.60

Factor	Factor Classes	Number of points	% of points	Class Area	% class area	Frequency Ratio	RF	RF*logRF
	AMPHIBOLITE	0	0.00	22652	0.26	0.00	0.00	0.00
LITHOLOGY	AMPHIBOLITE AND META-NORITE	0	0.00	207657	2.38	0.00	0.00	0.00
	BASAL CONGLOMERATE AND MASSIVE QUARTZITE	900	0.63	31039	0.36	1.76	0.02	-0.03
	BASIC META-VOLCANICS	25200	17.61	726389	8.34	2.11	0.02	-0.03
	BASIC ROCK	0	0.00	506652	5.82	0.00	0.00	0.00
	BIOTITE, HORNBLENDE GRANITE	34200	23.90	913150	10.49	2.28	0.02	-0.03
	CALC SILICATE, , QUARTZITE, SCHIST, MARBLE BAND	0	0.00	1089	0.01	0.00	0.00	0.00
	CARB. SHALE, SILTSTONE, SANDSTONE WITH NODULES	34200	23.90	569413	6.54	3.66	0.03	-0.05
	CARBONACEOUS PHYLLITE, QUARTZITE AND SCHIST	6300	4.40	69853	0.80	5.49	0.05	-0.06
	CHLORITE SCHIST, HORNBLENDE-ALBITE-ZOISITE SCHIST	14400	10.06	20560	0.24	42.62	0.37	-0.16
	EPIDIORITE	0	0.00	1992936	22.89	0.00	0.00	0.00
	GAR. MICA & CHLORITE SCHIST, QTZ WITH PHYLLITE	0	0.00	4622	0.05	0.00	0.00	0.00
	GLAUCONITIC SANDSTONE, SHALE WITH SILTSTONE BANDS	2700	1.89	19372	0.22	8.48	0.07	-0.08
	GNEISS, KYANITE SCHIST, QUARTZITE, CALC SILICATE	0	0.00	28985	0.33	0.00	0.00	0.00
	GRANITE	0	0.00	106411	1.22	0.00	0.00	0.00
	GRANITE GNEISS WITH RAFTS OF QUARTZITE, SCHIST	2700	1.89	802398	9.21	0.20	0.00	0.00
	GRANITE, GNEISS AND SCHIST	900	0.63	576540	6.62	0.09	0.00	0.00
	GRANULITE, GARNET MICA SCHIST, FELSPATHIC SCHIST	0	0.00	50452	0.58	0.00	0.00	0.00
	GRAVEL, PEBBLE, SAND, SILT AND CLAY	0	0.00	11474	0.13	0.00	0.00	0.00
	GREY NODULAR LIMESTONE & FOSSILIFEROUS LIMESTONE	4500	3.14	7454	0.09	36.74	0.32	-0.16
	GREY SAND, SILT	900	0.63	15506	0.18	3.53	0.03	-0.05

	AND CLAY							
	LIMESTONE WITH SHALE	0	0.00	1503	0.02	0.00	0.00	0.00
	LIMESTONE, DOLOMITE, SHALE, CARB. PHYLLITE/SLATE	0	0.00	6812	0.08	0.00	0.00	0.00
	LIMESTONE, SILTSTONE, MARL AND SHALE	12600	8.81	257839	2.96	2.97	0.03	-0.04
	MEDIUM TO COARSE GRAINED BIOTITE GRANITE	0	0.00	153713	1.77	0.00	0.00	0.00
	META BASICS SILLS AND DYKES	0	0.00	9699	0.11	0.00	0.00	0.00
	MIGMATITE GNEISS WITH MARBLE BANDS	0	0.00	14587	0.17	0.00	0.00	0.00
	ORTHOQUARTZITE WITH SHALE BANDS	0	0.00	4649	0.05	0.00	0.00	0.00
	PHYLLITE WITH CHLORITIC, GRAPHITIC & CARBONACEOUS	0	0.00	35225	0.40	0.00	0.00	0.00
	PHYLLITE, QTZ, SHALE, DOLOMITE, TUFF WITH DOLERITE	0	0.00	189	0.00	0.00	0.00	0.00
	PORPHYRITIC NONFOLIATED GRANITE	0	0.00	27540	0.32	0.00	0.00	0.00
	QUARTZ-SERICITE-CHLORITE SCHIST & LIMESTONE	0	0.00	55043	0.63	0.00	0.00	0.00
	QUARTZITE AND QUARTZ MICA SCHIST	0	0.00	5879	0.07	0.00	0.00	0.00
	QUARTZITE AND SLATE WITH BASIC METAVOLCANICS	0	0.00	139167	1.60	0.00	0.00	0.00
	QUARTZITE WITH HORNBLENDE-ALBITE-ZOISITE SCHIST	0	0.00	24909	0.29	0.00	0.00	0.00
	QUARTZITE, GARNETIFEROUS SCHIST AND PARAGNEISS	1800	1.26	42672	0.49	2.57	0.02	-0.04
	QUARTZITE, SHALE, PHYLLITE AND CONGLOMERATE	0	0.00	71722	0.82	0.00	0.00	0.00
	QUARTZITE, SLATE, LENSOIDAL LIMESTONE AND TUFF	0	0.00	80547	0.92	0.00	0.00	0.00
	SCHIST, GNEISS, MARBLE AND BASIC INTRUSIVES	0	0.00	33159	0.38	0.00	0.00	0.00
	SCHIST,AUGEN	0	0.00	1988	0.02	0.00	0.00	0.00

	GNEISS,QUARTZITE & AMPHIBOLITE							
	SCHISTOSE GRIT, SLATE, QUARTZITE WITH VOLCANICS	0	0.00	60060	0.69	0.00	0.00	0.00
	SERICITE QUARTZ SCHIST, CHLORITE SCHIST	0	0.00	4139	0.05	0.00	0.00	0.00
	SHALE WITH SHALY LIMESTONE	0	0.00	2546	0.03	0.00	0.00	0.00
	SHALE, QUARTZITE WITH CALCAREOUS NODULES	0	0.00	2923	0.03	0.00	0.00	0.00
	SILTSTONE, SHALE, LIMESTONE & CALCAREOUS SANDSTONE	0	0.00	901419	10.35	0.00	0.00	0.00
	SLATE, CARB. SHALE, QUARTZITE, SILTSTONE, PHYLLITE	1800	1.26	75368	0.87	1.45	0.01	-0.02
	SLATE, CARBO. SHALE, QUARTZITE, SILTSTONE PHYLLITE	0	0.00	9269	0.11	0.00	0.00	0.00
	UNMAPPED	0	0.00	1119	0.01	0.00	0.00	0.00
	Total	143100	100.00	8708289	100.00	113.97	1.00	-0.76

m	k	Ej
48	0.59	0.45

Factor	**Factor Classes**	**Number of points**	**% of points**	**Class Area**	**% class area**	**Frequency Ratio**	**RF**	**RF*logRF**	**Ej**	**1-Ej**
	0-1740.563	141300	98.74	4356108	50.02	1.97	0.97	-0.01		
DISTANCE FROM ROAD (in m)	1740.563-4389.248	1800	1.26	2007799	23.05	0.05	0.03	-0.04		
	4389.248-7794.699	0	0.00	1189357	13.66	0.00	0.00	0.00	0.08	0.92
	7794.699-12108.270	0	0.00	763012	8.76	0.00	0.00	0.00		
	12108.270-19297.556	0	0.00	392590	4.51	0.00	0.00	0.00		
	TOTAL	143100	100	8708866	100	2.03	1.00	-0.05		

m	k	Ej
5.00	1.43	0.08

Factor	Factor Classes	Number of points	% of points	Class Area	% class area	Frequency Ratio	RF	RF*logRF	Ej	1-Ej
	(-38.83)-(-6.25)	5400	3.77	382078	4.40	0.86	0.19	-0.14		
STREAM POWER INDEX	(-6.25)-(-2.03)	18000	12.58	1406132	16.18	0.78	0.17	-0.13		
	-2.03-0.688	40500	28.30	3206838	36.89	0.77	0.17	-0.13	0.98	0.02
	0.688-2.498	69300	48.43	2940930	33.83	1.43	0.31	-0.16		
	2.498-38.097	9900	6.92	756821	8.71	0.79	0.17	-0.13		
	TOTAL	143100	100.00	8692799	100.00	4.63	1.00	-0.68		

m	k	Ej
5.00	1.43	0.98

Factor	Factor Classes	Number of points	% of points	Class Area	% class area	Frequency Ratio	RF	RF*logRF	Ej	1-Ej
	(-6797.12)-(-5077.31)	0	0.00	143	0.00	0.00	0.00	0.00		
TOPOGRAPHIC WETNESS INDEX	(-5077.32)-82.105	143100	100.00	8640891	99.40	1.01	1.00	0.00		
	82.105-2505.470	0	0.00	51652	0.59	0.00	0.00	0.00	0.00	1.00
	2505.470-7274.028	0	0.00	63	0.00	0.00	0.00	0.00		
	7274.028-13137.008	0	0.00	50	0.00	0.00	0.00	0.00		
	TOTAL	143100	100.00	8692799	100.00	1.01	1.00	0.00		

m	k	Ej
5.00	1.43	0.00

Factor	Factor Classes	Number of points	% of points	Class Area	% class area	Frequency Ratio	RF	RF*logRF	Ej	1-Ej
	0-8163.579	48600	33.96	2183475	25.07	1.35	0.28	-0.15		
DISTANCE FROM RIVER (in m)	8163.579-17143.515	18000	12.58	2006681	23.04	0.55	0.11	-0.11		
	17143.515-26327.542	18000	12.58	1694265	19.45	0.65	0.13	-0.12	0.94	0.06
	26237.542-35715.658	41400	28.93	1563608	17.95	1.61	0.33	-0.16		
	35715.658-52042.816	14400	10.06	1260721	14.48	0.70	0.14	-0.12		
	TOTAL	140400	98.11	8708750	100.00	4.85	1.00	-0.66		

m	k	Ej
5.00	1.43	0.94

Factor	Factor Classes	Number of points	% of points	Class Area	% class area	Frequency Ratio	RF	RF*logRF	Ej	1-Ej
	654.844-2023.672	121500	84.91	1757348	20.18	4.21	0.85	-0.06		
ELEVATION (in m)	2023.672-3025.136	21600	15.09	1783202	20.48	0.74	0.15	-0.12		
	3025.136-4122.267	0	0.00	1409342	16.18	0.00	0.00	0.00	0.26	0.74
	4122.267-5127.360	0	0.00	1996202	22.92	0.00	0.00	0.00		
	5127.360-7777.557	0	0.00	1762677	20.24	0.00	0.00	0.00		
	TOTAL	143100	100.00	8708771	100.00	4.94	1.00	-0.18		

m	k	Ej
5.00	1.43	0.26

Table 5.4: Individual weights of each landslide causative factor (SE)

Factor	**1-Ej**	**Wi**
Slope	0.09	0.02
Aspect	0.02	0.01
Curvature	0.02	0.01
Lithology	0.55	0.14
Distance from Lineament	0.4	0.10
Distance from Road	0.92	0.24
Distance from River	0.06	0.02
SPI	0.02	0.01
TWI	1	0.26
Elevation	0.74	0.19
Total	3.82	

CHAPTER 6-RESULTS AND DISCUSSIONS

6.1 Landslide Susceptibility Map (LSM) Generation and classification

As mentioned earlier, The maps depicting the zones of landslide susceptibility were created using equations (5.4) and (5.7) by the incorporation of the raster calculator tool after reclassifying each landslide causative factor. The landslide susceptibility maps prepared after the application of the aforementioned models are shown in the following figures 6.1 and 6.2. The resulting Landslide Susceptibility Indices were classified into five susceptibility classes (Very Low, Low, Moderate, High and Very High) as shown in figures 6.1 and 6.2

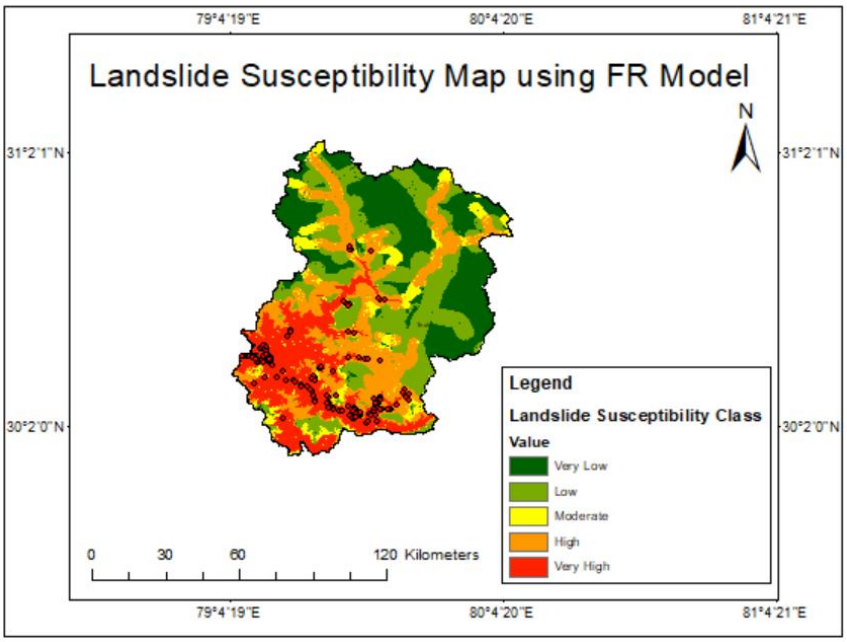

Fig. 6.1 Landslide Susceptibility Map for Frequency Ratio (FR) model

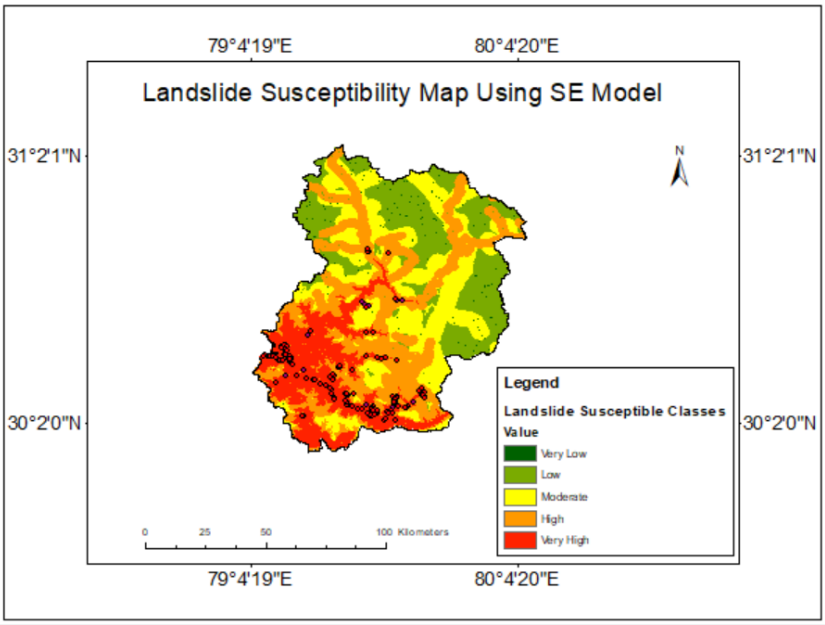

Fig. 6.2 Landslide Susceptibility Map (LSM) for Shannon Entropy (SE) model

6.2 Validation results

In this research study, the landslide susceptibility maps generated by the applied models namely frequency ratio and Shannon entropy were validated through receiver operating characteristics curve using the area under curve approach. Here, the landslide data points present in the training (80% points) and testing (20% points) datasets were used for plotting the ROC curve using the "ROC Tool" in GIS.

6.2.1 Area Under the Curve (AUC) of Receiver Operator Characteristics (ROC) curve

The Receiver Operator Characteristics (ROC) analysis is a cut-off independent accuracy metric that has various applications and is widely incorporated for the validation purpose in geology (Corominas et al. 2014). The value of the area under the curve (AUC) lies within the range of 0.5 to 1. The higher the value of AUC, the higher will be the accuracy of the predicted result (Pham et al. 2018).

In a ROC curve, True Positive Rate (TPR) and False Positive Rate (FPR) are plotted Equations 6.7 and 6.8 represent the numerical formula used for the determination of true positive and false-positive rates.

$$TPR = \frac{TRUE\ POSITIVES(TP)}{TP + FALSE\ NEGATIVES(FN)} \tag{6.1}$$

$$FPR = \frac{TRUE\ NEGATIVES(TN)}{TN + FALSE\ NEGATIVES(FP)} \tag{6.2}$$

Where,

TP & TN = pixels correctly classified as landslide and non-landslide

FP & FN = pixels incorrectly classified as landslide and non-landslide

Using the ROC tool, the success rate curve (SRC) was generated using the training dataset and the prediction rate curve (PRC) was generated using the testing dataset.

The different success rate and prediction rate curves for the four adopted models can be seen in Fig. 6.7 and 6.8 respectively.

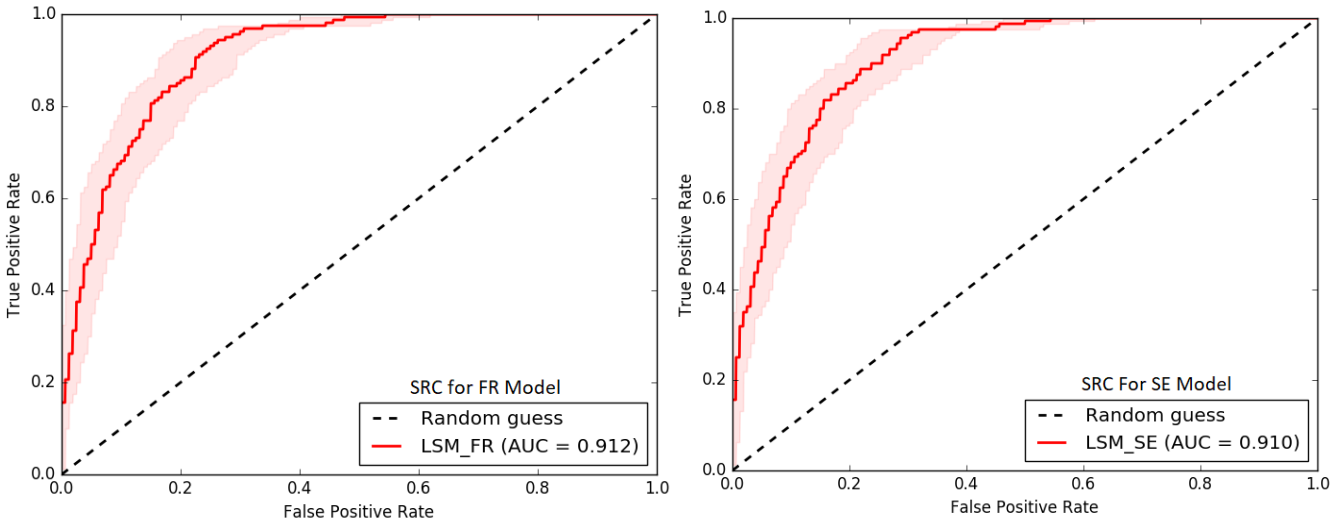

Fig. 6.1.1 Success rate curves for the FR and SE models

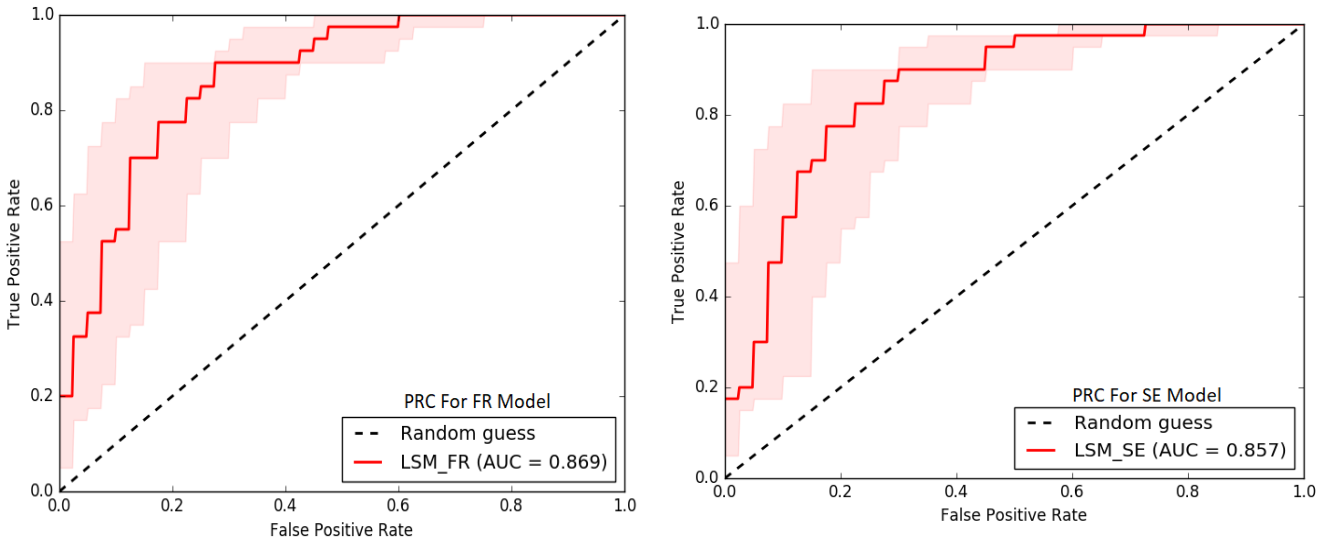

Fig. 6.1.2 Prediction rate curves for the FR and SE Models

From success rate curves and prediction rate curves, it can be easily seen that the values of AUC for the landslide susceptibility map generated by the frequency ratio model are higher than the AUC values for the landslide susceptibility map generated by the Shannon entropy model.

Table 6.1 Summary of ROC results for FR and SE Model

TYPE OF CURVE	AUC VALUE FOR FR MODEL	AUC VALUE FOR SE MODEL
Success Rate Curve	0.912 or 91.2%	0.910 or 91%
Prediction Rate Curve	0.869 or 86.9%	0.857 or 85.7%

CHAPTER 7- CONCLUSION, LIMITATION AND RECOMMENDATION

7.1 Conclusion

Landslide susceptibility mapping is defined as the art of mapping the zones of landslide susceptibility in a given area. This mapping should be done at regular intervals to keep the planners and designers in that area updated about the possibility of landslide occurrence in that area in the future so that they will ensure a disaster resilient infrastructure in that area. Landslide events can occur due to a number of reasons like extreme rainfall, unplanned infrastructure development, earthquake, volcanos, etc and their nature of occurrence is highly complex. Therefore, there is no definite solution to predict the landslides with a 100 percent accuracy.

In this research study, we applied two statistical models namely Frequency Ratio and Shannon Entropy for the prediction of landslide susceptibility in Chamoli District of Uttarakhand, India. Uttarakhand attracts a lot of tourism and tourism due to the state's natural scenic landscapes and religious importance. For the preparation of the landslide susceptibility map for the study area, a total of 200 landslide points were considered in the landslide inventory and out of them, 80% of the points (160 nos.) were taken as the points in the training dataset and the remaining 20% (40 nos.) of the points in landslide inventory were taken in the testing dataset.

A total of 10 landslide causative factors namely Slope, Elevation, Aspect, Curvature, Lithology, Topographic Wetness Index (TWI), Stream Power Index (SPI), Distance to Roads, Distance to River and Distance to lineament. All these landslide causative factors were reclassified and the area under these causative factors which includes the training dataset was computed through the "Tabulate Area" tool in GIS software. Afterward, FR and SE models were applied on the obtained data on MS-Excel and are utilized for the prediction of landslide susceptibility maps for the area.

Any research work without concrete validation becomes unfit for the application. For the validation purpose of the landslide susceptibility maps generated, we used Receiver

Operating Characteristic (ROC) curve approach and computed Area Under Curve (AUC) in GIS software through the ROC tool present in GIS software.

The methods utilised to produce landslide susceptibility maps were probabilistic statistical models that were not based on the opinion of any expert. Therefore, it can be easily inferred that the models incorporated in this research study can be easily applied in areas having similar features.

7.2 Limitations

Some of the limitations outlined in this study are:

- It is also seen that earthquake and excessive rainfall also initiates landslide in an area. However, these factors were not considered in this research study.
- Only bivariate methods were considered in this research study. However, landslides have a multivariate nature and the inter-relationship between the causative factors as well as landslide occurrence could have been done to increase the applicability of the research which has not been done.
- A field visit to the area could not be done due to travel restrictions. In fact, the cost of geotechnical field testing in the mountainous region of Chamoli district in Uttarakhand will be very high.
- LiDAR data have a much higher resolution as compared to the satellite imagery and could have been much better for producing a more detailed landslide susceptibility map. However, conducting a LiDAR survey is a very expensive process and requires highly specialized experts and equipment.

REFERENCES

A. D. Regmi, K. Yoshida, H. R. Pourghasemi, M. R. Dhital, and B. Pradhan, “Landslide susceptibility mapping along Bhalubang-Shiwapur area of mid-western Nepal using frequency ratio and conditional probability models,” *Jour. Mountain Sci.*, vol. 11, no.5, pp. 1266-1285, 2014.

A. Yalcin, “GIS-based landslide susceptibility mapping using analytical hierarchy process and bivariate statistic in Ardesen (Turkey): comparison of results and confirmations,” *Catena*, vol.72, pp. 1–12, 2008.

A. Yalcin, S. Reis, A.C. Aydinoglu and T. Yomralioglu, “A GIS-based comparative study of frequency ratio, analytical hierarchy process, bivariate statistics and logistic regression methods for landslide susceptibility mapping in Trabzon, NE Turkey,” *Catena*, vol. 85, pp. 274–287, 2011.

A.X. Zhu, R.X. Wang, J.P. Qiao, C.Z. Qin, Y.B. Chen, J. Liu, F. Du, Y. Lin and T.X. Zhu, “An expert knowledge-based approach to landslide susceptibility mapping using GIS and fuzzy logic,” *Geomorphology*, vol. 214, pp. 128–138, 2014.

B. T. Pham, I. Prakash, K. Khosravi, K. Chapi, P. T. Trinh, T. Q. Ngo, S. V. Hosseini and D. T. Bui, “A Comparison of Support Vector Machines and Bayesian Algorithms for Landslide Susceptibility Modeling”, *Geocarto International*, 2018.

C. Audisio, G. Nigrelli and G. Lollino, “A GIS tool for historical instability processes data entry: an approach to hazard management in two Italian Alpine River Basins.,” *Comput. Geosci.*, vol. 35, pp. 1735–1747, 2009.

C. Polykretis, C. Chalkias and M. Ferentinou, “Adaptive neuro-fuzzy inference system (ANFIS) modeling for landslide susceptibility assessment in a Mediterranean hilly area,” *Bull. Eng. Geol. Environ.*, vol. 78, pp. 1173–1187, 2019.

C.E. Shannon, “A Mathematical Theory of Communication”, *Bell Sys. Tech. Jour*., vol. 27, no. 3, pp. 379-423, 1948.

C.F. Chung and A.G. Fabbri, “Validation of Spatial Prediction Models forLandslide Hazard Mapping,” *Natural Hazards*, vol. 30, no.3, pp. 451-472, 2003.

C.I. Das, “Spatial statistical modelling for assessing landslide hazard and vulnerability.” Ph.D. Dissertation, Fac. Geo Info. Sci. Ear. Obs., University of Twente, Enschede, Netherlands, 2011.

C.J.V. Westen, E. Castellanos and S.L. Kuriakose, “Spatial data for landslide susceptibility, hazard, and vulnerability assessment: An overview,” *Engineering Geology*, vol. 102, no. 3-4, pp. 112-131, 2008.

C.Y. Chen and F.C. Yu, “Morphometric analysis of debris flows and their source areas using GIS,” *Geomorphology*, vol. 129, no. 3–4, pp. 387–397, 2011.

D. Ehret, J. Rohn, C. Dumperth, S. Eckstein, S. Ernstberger, K. Otte, R. Rudolph, J. Wiedenmann, “Frequency ratio analysis of mass movements in the Xiangxi Catchment, Three Gorges Reservoir Area, China,” *J. Earth Sci.*, vol. 21, pp. 824–834, 2010.

D. M. Cruden and D. J. Varnes, “Landslide types and processes,” in *Landslides: Investigation and Mitigation*, Transportation Research Board Special Report, 1996, pp. 36-75.

D. Myronidis, C. Papageorgiou, S. Theophanous, “Landslide susceptibility mapping based on landslide history and analytic hierarchy process (AHP),” *Nat. Hazards*, vol. 81, no. 1, pp. 245–263, 2016.

D. Pathak, “Knowledge based landslide susceptibility mapping in the Himalayas,” *Geoenvironmental Disasters*, vol. 3, no.8, 2016.

D.J. Varnes, “Slope movement types and processes,” Transp. Res. Board Spec. Rep. 1978, 176, 11–33.

E. Nohani, M. Moharrami, S. Sharafi, K. Khosravi, B. Pradhan, B.T. Pham, S. Lee and A.M. Melesse, “Landslide Susceptibility Mapping Using Different GIS-Based Bivariate Models,” *Water*, vol. 11, no. 7, 2019.

F. Guzzetti, A. C. Mondini, M. Cardinally, F. Fiorucci, M. Santangelo and K. T. Chang, "Landslide inventory maps: New tools for an old problem," *Earth-Science Reviews,* vol. 112, no. 1-2, pp. 42-66, 2012.

G. Paliaga, F. Luino, L. Turconi and F. Faccini, "Inventory of geo-hydrological phenomena in Genova municipality (NW Italy)," *Journal of Maps,* vol.15, no.4, pp. 1-11.

G. Zhang, Y. Cai, Z. Zheng, J. Zhen, Y. Liu, K. Huang, "Integration of the statistical index method and the analytic hierarchy process technique for the assessment of landslide susceptibility in Huizhou, China," *Catena,* vol. 142, pp. 233–244, 2016.

H. R. Pourghasemi, Biswajeet Pradhan, Candan Gokceogluand K. Deylami Moezzi, "Landslide Susceptibility Mapping Usinga Spatial Multi Criteria Evaluation Modelat Haraz Watershed, Iran," in *Terrigenous Mass Movements,* Springer-Verlag Berlin, Heidelberg, pp.23-49, 2012.

H. R. Pourghasemi, M. Mohammady and B. Pradhan, "Landslide susceptibility mapping using index of entropy and conditional probability models in GIS: Safarood Basin, Iran," *Catena,* vol. 97, pp. 71-84, 2012.

H. Shahabi, S. Khezri, B.B. Ahmad and M. Hashim, "Landslide susceptibility mapping at central Zab basin, Iran: a comparison between analytical hierarchy process, frequency ratio and logistic regression models," *Catena,* vol. 115, pp. 55–70, 2014.

H.R. Pourghasemi, B. Pradhan, C. Gokceoglu, and K.D. Moezzi, "A comparative assessment of prediction capabilities of Dempster–Shafer and weights-of-evidence models in landslide susceptibility mapping using GIS," *Geomatics Natural Hazards and Risk,* vol. 4, no. 2, pp. 93–118, 2013b.

H.R. Pourghasemi, H.R. Moradi, and S.F. Aghda, "Landslide susceptibility mapping by binary logistic regression, analytical hierarchy process, and statistical index models and assessment of their performances," *Natural Hazards,* vol. 69, no. 1, pp. 749–779, 2013a.

I. Yilmaz and I. Keskin, “GIS based statistical and physical approaches to landslide susceptibility mapping (Sebinkarahisar, Turkey),” *Bull. Eng. Geol. Environ.*, vol. 68, pp. 459–471, 2009.

I. Yilmaz, “Landslide susceptibility mapping using frequency ratio, logistic regression, artifcial neural networks and their comparison: a case study from Kat landslides (Tokat-Turkey)” *Comput. Geosci.*, vol. 35, pp. 1125–1138, 2009.

I. Yilmaz, I. Keskin, “GIS based statistical and physical approaches to landslide susceptibility mapping (Sebinkarahisar, Turkey),” *Bull. Eng. Geol. Environ.*, vol. 68, pp. 459–471, 2009.

J. Choi, H.J. Oh, H.J. Lee, C. Lee and S. Lee, “Combining landslide susceptibility maps obtained from frequency ratio, logistic regression, and artifcial neural network models using ASTER images and GIS” *Eng. Geol.*, vol. 124, pp. 12–23, 2012.

J. Corominas, C. J. van Westen, P. Frattini, L. Cascini, J. P. Malet, S. Fotopoulou, F. Catani, M. Van Den Eeckhaut, O. Mavroulli, F. Agliardi, K. Pitilakis, M. G. Winter, M. Pastor, S. Ferlisi, V. Tofani, J. Hervas and J. T. Smith, “Recommendations for the quantitative analysis of landslide risk,” *Bull. Eng. Geol. Eniron.*, vol. 73, no. 2, pp. 209-263, 2014.

J.H. Lee, M. I. Sameen, B. Pradhan, H.J. Park, “Modeling landslide susceptibility in data-scarce environments using optimized data mining and statistical methods,” *Geomorphology*, vol. 303, pp. 284-298, 2017.

J.P. Wilson and J.C. Gallant, “Digital terrain analysis” in *Terrain Analysis: Principles and Applications*, John Wiley and Sons, pp. 1–27, 2000.

M. Meinhardt, M. Fink and H. Tunschel, “Landslide susceptibility analysis in central Vietnam based on an incomplete landslide inventory: comparison of a new method to calculate weighting factors by means of bivariate statistics,” *Geomorphology*, vol. 234, pp. 80–97, 2015.

M. Mohammady, H.R. Pourghasemi and B. Pradhan, “Landslide susceptibility mapping at Golestan Province, Iran: a comparison between frequency ratio, Dempster-Shafer, and weights-of-evidence models,” *J. Asian Earth Sci.*, vol. 61, pp. 221–236, 2012.

M. Motamedi, “Quantitative landslide hazard assessment in regional scale using statistical modelling techniques,” Ph.D. Dissertation, Gr. Fac., University of Akron, Akron, Ohio, The United States of America, 2013.

R.G. Rejith, S. Anirudhan and M. Sundararajan, “Delineation of Groundwater Potential Zones in Hard Rock Terrain Using Integrated Remote Sensing, GIS and MCDM Techniques: A Case Study from Vamanapuram River Basin, Kerala, India” in *GIS and Geostatistical Techniques for Groundwater Science*, Elsevier, 2019.

Radha Raman and Milap Punia, “The application of GIS-based bivariate statistical methods for landslide hazards assessment in the upper Tons-river valley, Western Himalaya, India,” *Georisk*, vol. 6, no. 3, pp. 145-161, 2012.

S. Chauhan, M. Sharma and M.K. Arora, “Landslide susceptibility zonation of the Chamoli region, Garhwal Himalayas, using logistic regression model,” *Landslides,* vol. 7, pp. 411-423, 2010.

S. Lee and B. Pradhan, “Probabilistic landslide hazards and risk mapping on Penang Islands, Malaysia,” *J. Earth. Syst. Sci.*, vol. 115, pp. 661–672, 2006.

S. Lee, “Geological application of geographic information system,” *Korea Inst. Geosci. Min. Resour*., vol. 9, pp. 109–118, 2014.

S. Lee, B. Pradhan, “Probabilistic landslide risk mapping at Penang Island, Malaysia,” *J Earth Syst. Sci.*, vol. 115, no. 6, pp. 661–672, 2006.

S. Mandal and S. Mondal. “Probabilistic approaches and landslide susceptibility” in *Geoinformatics and modelling of landslide susceptibility and risk*, Environmental science and engineering, Springer book series (ESE), pp 145–163, 2019.

S.E. Autade, S.D. Pardeshi, “Assessment of lithology and geomorphic control on slope instability in Raigad District, Maharashtra” *J. Geol. Soc. India*, vol. 90, no. 3, pp. 283–288, 2017.

Sangeeta, B. K. Maheshwari and D.P. Kanungo, “GIS-based pre- and post-earthquake landslide susceptibility zonation with reference to 1999 Chamoli earthquake,” *J. Earth Syst. Sci*., vol. 129, 2019.

T.H. Mezughi, J.M. Akhir, A.G. Rafek and I. Abdullah, “Landslide susceptibility assessment using frequency ratio model applied to an area along the E-W Highway (Gerik-Jeli),” *Am. J. Environ. Sci*., vol. 7, pp. 43–50, 2011.

U. Kamp, B.J. Growley, G.A. Khattak and L.A. Owen, “GIS-based landslide susceptibility mapping for the 2005 Kashmir earthquake region,” *Geomorphology*, vol. 101, pp. 631–642, 2008.